Meng et al. Biochar (2026) 8:83
https://doi.org/10.1007/s42773-026-00598-9

Biochar

ORIGINAL RESEARCH Open Access

Biochar orchestrates coordinated soil-microbe-metabolite responses in acidifying paddy soils: evidence from a 5-year field study

Jun Meng[1], Zhonghua Cui[1,7], Zhangtao Li[1], Jiaxin Li[2*], Minjun Hu[3], Jun Xu[3], Zhiyuan Yao[4], Caixian Tang[5], Dong Yang[6], Alexandru Ozunu[7], Shengdao Shan[1] and Huaihai Chen[2*]

Abstract

Biochar is increasingly recognized for its capacity to remediate acidifying soils, but the mechanisms through which it achieves long-term effects remain poorly understood. This five-year field study examined how biochar's effects on soil chemistry propagate through biological systems to reshape soil function. We conducted a randomized field experiment comparing three biochar application rates (4.5, 11.25, and 22.5 t ha^{-1}) with lime and swine manure in an acidic paddy soil. Integrated soil microbiome, metagenomic, metaviromic, and metabolomic analyses assessed how amendments altered soil properties and their associations with microbial communities and metabolic functions. All amendments alleviated acidification (pH increased from 5.5 to 6.4) and reduced exchangeable aluminum (from 12.5 to 3.5 mg kg^{-1}). High-dose biochar (22.5 t ha^{-1}) initiated a mechanistic cascade absent under traditional amendments: improved soil chemistry drove restructuring of prokaryotic and viral communities toward nutrient-cycling phenotypes (enriching Chloroflexi, Planctomycetota, Algavirales, and Crassvirales), which in turn reshaped metagenomic functions and soil metabolite profiles. Specifically, biochar elevated genes related to nutrient exchange and cell–cell interactions while enriching lipids and terpenoids that support plant growth and long-term carbon stabilization. This coordinated restructuring of soil chemistry, microbial communities, and metabolic function did not occur under lime or manure. The findings demonstrate that biochar's long-term superiority emerges from orchestrating sequential changes across the soil-microbe-metabolite system as an integrated whole. This mechanistic understanding provides novel insights for deploying biochar as an ecosystem restoration tool in acidifying agricultural systems.

Highlights

- Biochar initiated a chemistry-community-function cascade in acidic soil.
- This coordinated cascade did not occur under lime or manure amendments.
- Biochar elevated soil pH and suppressed metals, favoring nutrient-cycling taxa.
- Biochar-enriched microbial communities enhanced nutrient exchange and signaling.
- Biochar restructured soil metabolites toward lipids and terpenoids for stability.

*Correspondence:
Jiaxin Li
lijx393@mail2.sysu.edu.cn
Huaihai Chen
chenhh68@mail.sysu.edu.cn
Full list of author information is available at the end of the article

Springer

Keywords Biochar, Mechanistic cascade, Soil-microbe-metabolite interface, Acidic soil remediation, Microbial communities, Metabolomics

Graphical Abstract

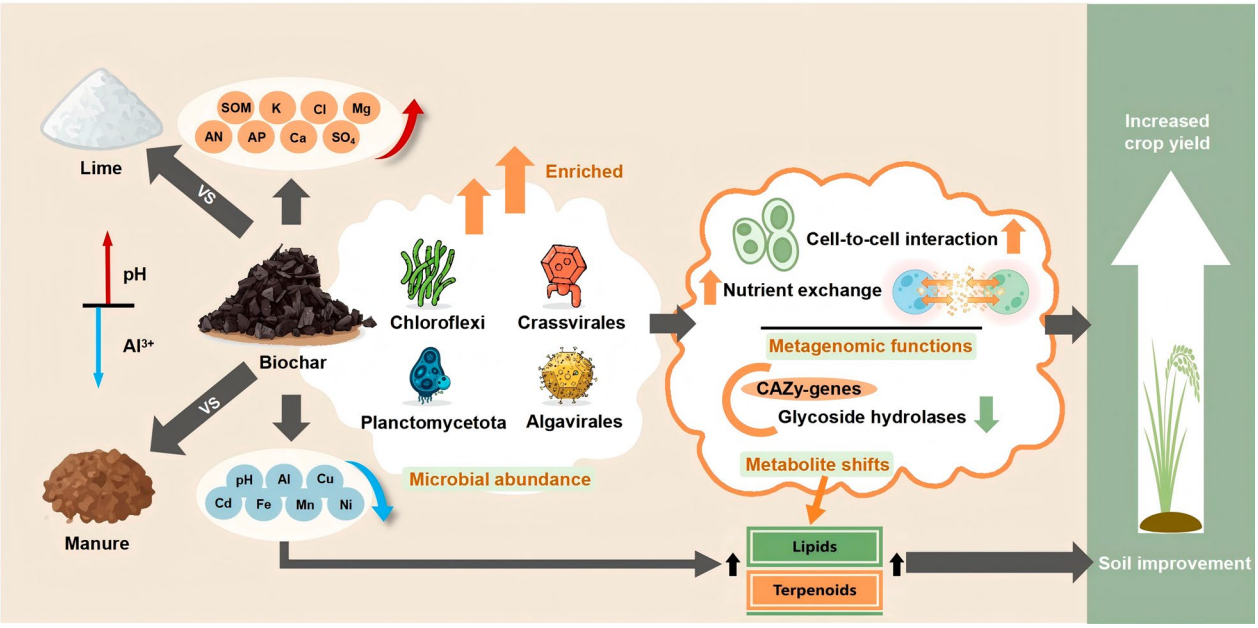

1 Introduction

Soil serves as the cornerstone of terrestrial ecosystem function, underpinning global food security, biogeochemical cycling, climate mitigation, and biodiversity (Bunemann et al. 2018). However, unsustainable agricultural practices, such as intensive monocropping and the excessive application of chemical fertilizers, have accelerated land degradation on a global scale (Liu et al. 2021). Among these threats, soil acidification has emerged as a particularly pressing issue, leading to nutrient depletion, increased heavy metal availability, reduced crop yields, and suppressed microbial activity (Li et al. 2023). Traditional amendments such as lime and animal manure are commonly used to neutralize soil acidification. Lime directly neutralizes soil exchangeable H^+ or Al^{3+}, while animal manures detoxify Al^{3+} and increase soil organic matter and nutrient supply (Fu et al. 2022). However, the application of lime and animal manure is constrained. The ameliorative effects of lime are often transient and can induce cation imbalances (Hu et al. 2016a, b), while animal manures risk introducing heavy metals and pathogens, posing potential threats to food safety and human health (Nicholson et al. 1999). Therefore, selecting sustainable amendments that provide effective, long-term soil improvement without adverse effects is crucial for global agricultural resilience.

Biochar, a carbon-rich material, has gained prominence as a promising soil amendment (Chen et al. 2019). Its alkaline nature, porous structure, and rich nutrient concentrations can improve soil pH, structure, and fertility, making it particularly suitable for the remediation of acid soils (Biederman and Harpole 2013). Unlike lime or animal manure, biochar exhibits superior structural stability and environmental persistence, serving as a persistent carbon sink while continuously enhancing soil fertility (Lehmann 2007). Its high surface area and adsorption capacity further aid in nutrient retention and contaminant immobilization (Yao et al. 2012). Despite these acknowledged benefits, the current understanding has predominantly focused on short-term agronomic outcomes, such as immediate shifts in soil pH and crop yield. There remains a lack of consensus and clear mechanistic understanding regarding the long-term effects of biochar on holistic soil ecological functions, especially its sustained influence on soil biodiversity and key microbial-driven recovery processes (Kerner et al. 2023). Furthermore, while the dose-dependent effect of biochar is acknowledged (Zhao et al. 2024), the ecological

thresholds, trade-offs, and mechanistic drivers across application gradients remain poorly understood, limiting the development of optimized remediation strategies.

Soil microorganisms are central agents in ecosystem functioning, governing organic matter decomposition, nutrient cycling, and soil health (Trivedi et al. 2020). Their communities are sensitive indicators of soil condition and are directly influenced by amendments (Kerner et al. 2023), particularly during the remediation of acid soils (Fierer et al. 2021). Biochar can alter microbial habitats and metabolic activities, often reducing acidophilic taxa while stimulating groups involved in nutrient cycling (Palansooriya et al. 2019; Chen et al. 2022). However, these responses are complex and context-dependent: higher application rates may increase microbial biomass and enrich nutrient-cycling taxa, yet sometimes reduce α-diversity due to stronger environmental filtering (Li et al. 2019). Critically, most evidence comes from short-term or controlled-environment experiments, leaving a scarcity of field-based, long-term data on how microbial communities and their functional capacities evolve under sustained biochar application in acid soils.

A more notable research gap concerns the soil virome. Viruses, particularly bacteriophages, are increasingly recognized as important regulators of microbial communities and biogeochemical processes, influencing host metabolism, stress resistance, and ecosystem functioning through mechanisms such as lysis and horizontal gene transfer (Kuzyakov and Mason-Jones 2018). It has been shown that viral activity affects microbial turnover and functional traits, including responses to soil acidity and heavy metal stress (Santos-Medellín et al. 2022). However, previous studies examining how soil viral communities respond to long-term application of biochar under field conditions remain very limited. This lack of investigation leaves a substantial gap in understanding the full scope of biochar-induced biological changes in soil ecosystems. Therefore, a systematic investigation into the long-term effects of biochar applied at varying rates, particularly from an integrated microbial and viral perspective, is needed to better elucidate ecological responses to soil amendments and to advance mechanistic understanding of how biochar enhances soil biochemical functioning.

To address these research gaps, we conducted a five-year field experiment in acidic paddy soils of Southeast China. Specifically, we asked whether long-term biochar application, particularly at higher rates, outperforms traditional amendments by fundamentally restructuring the soil microbiome and metabolic functions in ways that transcend simple chemistry. To systematically address this question, we compared biochar applied at three rates (4.5, 11.25, and 22.5 t ha^{-1}) with conventional amendments using integrated amplicon sequencing, metagenomics, metaviromics, and metabolomics. This multi-omics approach enabled us to examine whether changes in soil chemistry, microbial communities, and metabolic functions operate in concert under biochar amendment. We hypothesized that biochar-induced improvements in soil chemistry drive restructuring of prokaryotic and viral communities, which in turn reshape metabolic pathways supporting nutrient and carbon cycling. Specifically, we predicted that (1) high-dose biochar would exceed lime and swine manure in improving soil fertility and reducing metal bioavailability; (2) biochar would induce dose-dependent shifts in prokaryotic and viral communities correlating with improved soil chemistry; and (3) these community changes would manifest as metagenomic and metabolomic shifts toward nutrient acquisition and carbon stabilization pathways. By unraveling the mechanistic interplay among soil chemistry, microbial ecology, and metabolic functions, this study provides critical multi-omics insights essential for developing optimized management strategies in acidifying paddy soils.

2 Materials and methods

2.1 Study site and experimental design

The field experiment site was located in Xintong county, Hangzhou, Zhejiang province, China (119.82°E, 29.91°N). This region experiences a subtropical monsoon humid climate with a mean annual precipitation of 1523 mm and an average annual temperature of 17.2 ℃. The soil had pH 5.43 ± 0.05, organic matter 22.1 ± 0.4 g kg^{-1}, exchangeable Al^{3+} 2.14 ± 0.12 cmol kg^{-1}, exchangeable H^{+}1.05 ± 0.08 cmol kg^{-1}, cation exchange capacity (CEC) 7.86 ± 0.35 cmol kg^{-1}, available P 3.62 ± 0.16 mg kg^{-1}, total Cd 0.57 ± 0.04 mg kg^{-1}, and $CaCl_2$-extractable Cd 0.21 ± 0.05 mg kg^{-1}. Its texture was silt clay loam with 26% sand, 52% silt, and 22% clay.

The field experiment commenced in May 2019 to evaluate the effect of soil amendments on alleviating soil acidification and Cd contamination. Previous studies have reported that biochar application rates typically range from 5 to 10 t ha^{-1}, and occasionally extend to 15 t ha^{-1}, depending on soil type and agronomic objectives (Urgessa 2021; Frimpong et al. 2025). To align with common agricultural practice while enabling systematic dose–response analysis, we selected three application rates: a medium dose of 11.25 t ha^{-1} (within the typical range), supplemented with a low dose of 4.5 t ha^{-1} (representing 40% of the conventional range) and a relatively high dose of 22.5 t ha^{-1} (approximately double the upper conventional rate). This gradient allows examination of ecological thresholds and trade-offs across the application spectrum. The experiment consisted of

eight treatments and three replicates in a randomized complete block design (Fig. S1). The eight treatments were non-amended control (CT), lime at 1.13 t ha^{-1} (L), swine manure at 2.25 t ha^{-1} (PM), swine manure at 2.25 t ha^{-1} and biochar at 4.5 t ha^{-1} (PMBC), low-dose biochar at 4.5 t ha^{-1} (BCL), medium-dose biochar at 11.25 t ha^{-1} (BCM), high-dose biochar at 22.5 t ha^{-1} (BCH), and biochar at 112.5 t ha^{-1} per five-year (equivalent to five-year cumulative BCH treatment) (BCF). All treatments (except for BCF) were applied annually before rice planting.

For the amendments, lime was purchased from a local farm (pH 9.59, 6.7% total C), and swine manure (pH 7.70, 24.7% C) was obtained from an intensive livestock production facility (Hangzhou, Zhejiang Province, Eastern China). The manure-derived biochar, produced by pyrolysis at 550–600 °C, was strongly alkaline (pH 10.75), with 31.1% total C, 53.7% ash, and a $CaCO_3$ equivalent of 20.2%, supplied by Jiangsu Benenv Environmental Technologies Co., Ltd. (Yixing, Jiangsu Province, China). Basic properties, including trace metal contents, are presented in Table S1.

Plots of 5 m × 4 m were arranged and concrete barriers (0.2 m wide, 0.2 m deep) were installed between plots to prevent cross-contamination (Fig. S1). All amendments were applied in conjunction with basal fertilizers of urea, diammonium phosphate, and potassium chloride, at rates of 180 kg N ha^{-1}, 40 kg P ha^{-1}, and 125 kg K ha^{-1}, respectively, and mixed into the top 15 cm. Ten days after amendment addition, 30-day-old seedlings of rice (*Oryza sativa* L.) were transplanted into the field plots with 18cm × 15 cm inter and intra row spacing.

2.2 Soil sample collection and property characterization

At the rice harvest on October 25, 2023, five cores (0–20 cm) were collected from each plot using a soil auger. Soil samples were kept on ice before being transported to the laboratory. The soil was then sieved through a 2-mm mesh and divided into two portions. One portion was air-dried for the determination of soil properties, nutrient and metal levels, while the other was frozen at −80 °C for subsequent DNA extraction and microbial analyses.

Soil pH, soil organic matter (SOM), total N (TN), available N (AN), available P (AP), CEC, chloride (Cl), sulfate (SO_4), available Si, exchangeable K, exchangeable Ca, and exchangeable Mg as well as bioavailable metals of Al, Cd, Cu, Fe, Mn, and Ni were determined. Soil pH was measured in 1:2.5 H_2O by a pH meter (S470, SevenExcellence™, Mettler-Toledo GmbH, Gießen, Germany). Soil CEC was determined using the ammonium acetate exchange method. Soil SOM was quantified by the $K_2Cr_2O_7$-H_2SO_4 oxidation method, with TN assessed using the Kjeldahl method (Kjeltec Analyzer CID-310, Foss, Sweden). Soil AP was measured using the molybdenum-antimony colorimetric method following extraction with ammonium chloride and hydrochloric acid (Murphy and Riley 1962). Soil AN was determined using the alkali-hydrolysis diffusion method with boric acid absorption (Dodor and Tabatabai 2019). For other nutrient ions, Cl was quantified by silver nitrate titration, and SO_4 by EDTA titrimetry. Soil exchangeable Ca, Mg, and K were detected by atomic absorption spectrophotometry after extraction in ammonium acetate, while available Si was measured by the citric acid extraction-molybdenum blue spectrophotometric method. Soil bioavailable metal ions were extracted with 0.1 mol L^{-1} $CaCl_2$ at a 1:10 (w/v) ratio and quantified using an Inductively Coupled Plasma-Optical Emission Spectrometer (ICP-OES) (iCAP 6300, Thermo Fisher Scientific, USA).

2.3 Soil microbiome analyses

Soil DNA was extracted from each sample (0.5 g) using the FastDNA Spin Kit (MP Bio, Solon, OH, USA) following the manufacturer's instructions, and then column-purified using the OneStep PCR Inhibitor Removal Kit (Zymo Research, Irvine, USA). The purity and concentration of DNA were assessed using the Nanodrop One (Thermo Fisher Scientific, MA, USA). The primer of 515F (5′-GTG CCA GCM GCC GCG GTA A-3′) and 907R (5′-CCG TCA ATT CMT TTR AGT TT-3′) was targeted for 16S V4 and V5 regions of soil prokaryotes (Biddle et al. 2008). Fungal ITS1 regions were amplified by applying the primer pair F (5′-CTT GGT CAT TTA GAG GAA GTA A-3′) and R (5′-GCT GCG TTC TTC ATC GAT GC-3′) (Gardes and Bruns 1993). The PCR amplification was performed using a BioRad S1000 PCR instrument (Bio-Rad Laboratory, CA, USA). Amplified PCR products were sequenced on the Illumina MiSeq platform (Illumina, San Diego, CA, USA) to generate 300 bp paired-end reads.

Paired-end reads were merged based on their overlap using USEARCH to obtain raw tags (Edgar 2010). Quality control of the raw tags to clean tags was performed using fastp (version 0.14.1) with a sliding-window quality trimming (-W 4 -M 20), with primers removed by Cutadapt (Chen 2023). The QIIME 2 pipeline (2022.11) was employed to further denoise the clean tags, clustering them into amplicon sequence variants (ASVs) through DADA2 (Callahan et al. 2016). Taxonomic classification of each ASV was performed using the Silva 16S reference database (version 138) for prokaryotic taxa and the UNITE ITS reference database (version 8.0) for fungal taxa (Abarenkov et al. 2024).

2.4 Soil metagenomics

According to the manufacturer's protocol, 1 μg of DNA was extracted from each soil sample using the NEB Next® Ultra™ DNA Library Prep Kit for Illumina (NEB, USA) to construct shotgun metagenomic sequencing libraries with indexing codes appended. Sequencing was then performed on the Illumina NovaSeq 6000 platform, generating 150 bp paired-end reads. The quality of the libraries was assessed using an Agilent Bioanalyzer equipped with a DNA7500 chip (Agilent, Santa Clara, USA), while concentrations were measured via the broad-range double-stranded DNA assay on an Invitrogen Qubit fluorometer (Invitrogen, Waltham, USA).

The raw reads obtained were subjected to quality control using Trimmomatic (version 0.36) to produce clean reads. Subsequently, de novo assembly of the clean reads was performed using MEGAHIT (v1.1.2) with k-mer sizes ranging from k-min 35 to k-max 95, stepping by 20 (Li et al. 2016). Open reading frames (ORFs) were predicted using Prodigal (Hyatt et al. 2010). Gene clustering and redundancy reduction were conducted by Linclust (Steinegger and Söding 2018). The longest sequence from each cluster was selected as the representative sequence, generating a non-redundant gene catalog (Unigenes). Clean reads were then mapped to the gene catalog using bbmap to calculate the abundance of each Unigene in the samples. Species annotation of the non-redundant Unigenes was performed via BLASTP (version 2.2.31 +) against the NCBI-NR (Non-Redundant Protein Sequence) database with an e-value threshold of ≤0.0001 (Altschul et al. 1990). Thus, species composition and abundance information for each taxonomic level were obtained, combined with the gene abundance table. Functional annotation was carried out by aligning the non-redundant Unigenes against the KEGG genes database (https://www.kegg.jp/) using DIAMOND (e-value ≤ 0.001) (Buchfink et al. 2015). Additionally, the CAZy database (http://www.cazy.org) was used for carbohydrate-active enzyme annotation, with the non-redundant Unigenes aligned against CAZyDB (version:2016.7.15) using hmmscan with an e-value threshold of ≤0.0001.

2.5 Soil metaviromics

A total of 0.60 g soil from each sample was suspended in 3 mL of pre-cooled sterile Stabilization Buffer (SB) and vortexed for 5 min. The mixture then underwent triplicate cycles of liquid nitrogen freezing and thawing, followed by centrifugation at 12,000 × g for 5 min. The supernatant was sequentially filtered through tangential flow filters of 0.45 μm and 0.22 μm, and then transferred to ultracentrifuge tubes containing 28% (w/w) sucrose. The tubes were centrifuged at 160,000 × g at 4 °C for 2 h using a Himac CP 100WX ultracentrifuge (Hitachi, Tokyo, Japan). The resulting pellet was resuspended in 200 μL of SB buffer, with Enzyme Mix Buffer and Enzyme Mix added proportionally. The mixture was then incubated at 37 °C for 60 min. Subsequently, Stop Solution (2 μL) was added to inactivate the enzymes by incubating at 65–75 °C for 10 min. The samples were centrifuged at 2000 rpm for 5 min to obtain the required supernatant.

Viral DNA was extracted from the samples using the Qiagen AllPrep PowerViral DNA/RNA Extraction Kit (Qiagen, Hilden, Germany), followed by the illustra Ready-To-Go GenomiPhi V3 DNA Amplification Kit (GE Healthcare, Amersham, UK) to carry out the whole genome amplification, and then metagenomic libraries were created using the ALFA-SEQ DNA Library Prep Kit (Magigene, Guangdong, China), according to the manufacturer's protocol. The prepared DNA libraries were sequenced on the Illumina platform, generating 150 bp paired-end reads.

The obtained raw data were processed to clean reads using Trimmomatic to remove adapters and filter out low-quality reads. These clean reads were then assembled into contigs using MEGAHIT. Subsequently, the assembled contigs were annotated for genes using the "Prodigal" encapsulated within CheckV software. These annotated gene fragments were then compared against the Hidden Markov Model (HMM) constructed from various viral databases, including KEGG, VOGDB, PfamA, PfamB, IMG/VR, TIGRFAM, RVDB, NCBI GenBank (viral), GVD, GPD, MGV, CHVD, and Riboviria, to differentiate genes of viruses from those of other microbes. Then, potential viral sequences were identified through sequence alignment (amino acid identity, AAI) and HMM profiling (Nayfach et al. 2021). The identification results from CheckV were validated using Virsorter2, and viral taxonomic annotations were performed using PhaGCN2 (Guo et al. 2021). Host prediction for the identified viruses was conducted using CHERRY (score > 0.9) and Prokaryotic virus Host Predictor (PHP, threshold set to 1,400) (Shang and Sun 2022). All sequencing raw data have been deposited in the NCBI Sequence Read Archive (SRA) under BioProject accession number PRJNA1102840.

2.6 Soil metabolomics

A total of 0.10 g soil from each sample was weighed and mixed with beads in 1 mL of extraction solvent (methanol: acetonitrile: water = 2:2:1, v/v/v) containing an isotopically labeled internal standard mixture. The mixed solution was vortexed for 30 s, homogenized for 4 min (35 Hz), and sonicated in an ice-water bath for 5 min three times. The mixture was then incubated at –40 °C for 1 h, followed by centrifugation at 12,000 rpm for

15 min at 4 °C with collected supernatants containing the extracted metabolites.

For determination of soil metabolite composition, LC–MS analyses were performed using an Ultra High Performance Liquid Chromatography (UHPLC) system (Vanquish, Thermo Fisher Scientific) with a Phenomenex Kinetex C18 (2.1 mm × 50 mm, 2.6 μm) for chromatographic separation of target compounds. This system was coupled to Orbitrap Exploris 120 mass spectrometer (Orbitrap MS, Thermo Fisher Scientific) to acquire MS/MS spectra in information-dependent acquisition (IDA) mode in the control of the acquisition software (Xcalibur, Thermo Fisher Scientific) (Alseekh et al. 2021). The raw data were converted to the mzXML format using ProteoWizard for subsequent metabolite identification. Throughout the identification process, stringent process and data quality controls were maintained using isotopically labeled internal standards, ensuring the reliability and accuracy of the experiments. Further processing of the original data set was performed following several meticulous processing steps including single peak filtering, missing data estimation, internal standard-based normalization, and a log data transformation previously reported in our studies (Fu et al. 2024; Huang et al. 2023).

2.7 Data analysis

For α-diversity, richness and Shannon index were calculated using the minimum sequence number obtained from all samples before rarefaction to 37,507 and 57,166 for prokaryotic and fungal communities, respectively. The β-diversity for the microbial community, function, and metabolites was assessed using Bray–Curtis distance, performed via the "vegan" R package (Dixon 2003). Differences in microbial taxa abundance were assessed using the Kruskal–Wallis test. Microbial community co-occurrence networks, as well as their topological coefficients, were constructed and calculated using the "ggClusterNet" package in R (Wen et al. 2022). Viral abundance was represented using RPKM (Reads Per Kilobase of genome per Million mapped reads). The "picante" R package was used to calculate NRI (Net Relatedness Index) and betaNRI (Kembel et al. 2010). One-way ANOVA was used to compare soil characteristics, NRI, and betaNRI differences among treatments. The structural distribution of soil microbial community composition, functional profile, and metabolite variation was evaluated using PERMANOVA (permutational multivariate analysis of variance), dbRDA (distance-based redundancy analysis), and DistLM (distance-based linear model analysis) analyses in PRIMER 7 (v7.0.13). The PCA (principal component analysis) and PERMANOVA were used to compare soil characteristics under different treatments for dimensionality reduction. The linear relationships between different soil properties under soil amendments were analyzed via Pearson's correlation analysis. The SEM (structural equation modeling) was facilitated by the use of the R package "piecewiseSEM" (https://github.com/cran/piecewiseSEM).

3 Results

3.1 Soil chemistry: biochar drives pH and nutrient improvements

Generally, five-year soil amendments improved soil basic properties and increased nutrient concentrations, while reducing bioavailable metal concentrations compared to the control (Fig. 1a). For example, all soil amendments except PM significantly increased soil pH from 5.5 to 6.4 on average ($p < 0.05$). While BCH and BCF increased SOM by 62% and 72%, respectively, all treatments except PM and BCF significantly reduced total N by an average of 31% ($p < 0.05$). While most soil amendments improved soil nutrient availability, BCH and/or BCF further increased available P, CEC, K, and Mg in comparison with others. Only available Si was reduced by PM, and K decreased in the L and PM treatments ($p < 0.05$). In addition, soil amendments lowered Al and Fe by 72% and 57%, respectively, on average ($p < 0.05$). Moreover, bioavailable Cd and Ni decreased in all treatments except PM ($p < 0.05$). In comparison, bioavailable Cu and Mn were less responsive to soil amendments. Specifically, all amendments except BCH decreased Cu bioavailability by an average of 22% ($p < 0.05$). Soil Mn bioavailability increased by an average of 47% in the PM, BCL, and BCF treatments but decreased by 24% in the L and BCM treatments ($p < 0.05$). Furthermore, BCF significantly increased crop yields by 12.4% compared to the control, outperforming both lime and swine manure treatments ($p < 0.05$; Table S2).

Principal component analysis (PCA) revealed clear separation in soil characteristics among the treatments (Fig. 1b, $p < 0.0001$). In particular, BCL, BCM, BCH, and BCF were distinct from the control and other treatments. The distribution of control and PM were positively related to bioavailable Al, Cd, Cu, Fe, and Ni, while BCM, BCH, and BCF was positively associated with soil pH, SOM, and CEC. Pearson's correlations also confirmed that soil basic properties and nutrient concentrations were positively associated with each other but negatively related to bioavailable metals except Mn (Fig. 1c, $p < 0.05$).

3.2 Prokaryotic and viral communities: community restructuring under biochar

Overall, most α-diversity parameters, e.g., richness and Shannon index, for both prokaryotes and fungi showed no significant differences among treatments (Fig. S2). However, five-year soil amendments caused notable

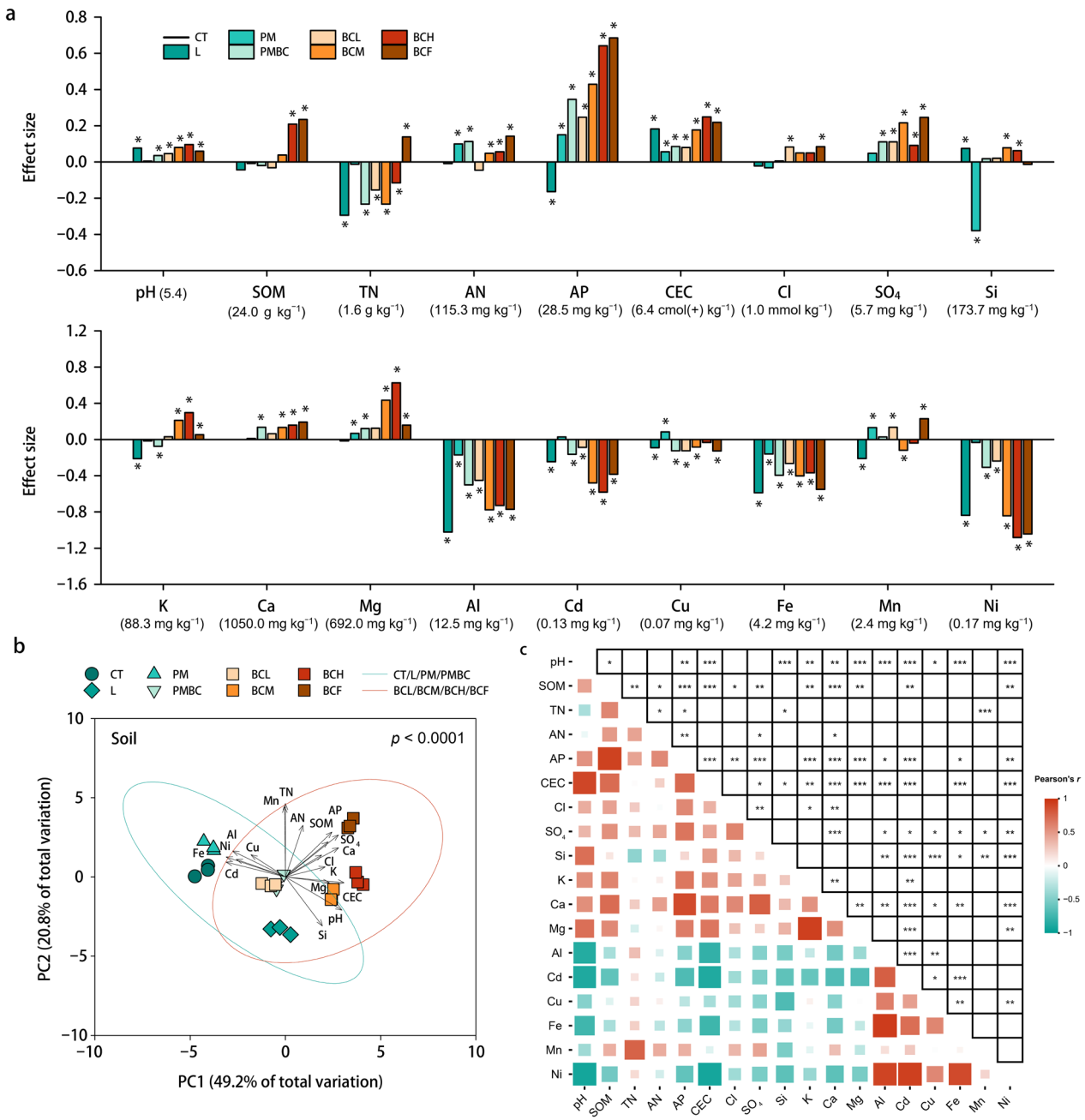

Fig. 1 **a** Soil characteristics; and **b** Principal component analysis (PCA) of soil characteristics under control (CT), lime (L), manure (PM), biochar with manure (PMBC), biochar at low (BCL), medium (BCM) and high dose (BCH), and biochar at 5-fold dose only in the first year (BCF); **c** Pearson correlation coefficients (*r*) showing relationships between soil characteristics across amendment treatments. The size and color of the squares represent the magnitude and direction of the correlations, respectively. The prediction ellipse in PCA indicates 95% confidence region. Vectors represent the explanatory variables of soil characteristics. The asterisk indicates significant differences of soil amendment treatments compared to CT ($p < 0.05$); Statistical significances of Pearson's correlations are represented as follows: $^{*}p < 0.05$; $^{**}p < 0.01$; $^{***}p < 0.001$

changes in the community structure of prokaryotes ($p = 0.0002$) but not fungi ($p = 0.3682$) (Fig. 2a). In the prokaryotic community, biochar treatments led to distinct separation from others, with positive correlations to exchangeable Mg, Ca and Si, and P availability but a negative correlation to soil bioavailable Al. In particular, pair-wise tests indicated significant differences of BCH and BCF from the control ($p < 0.05$), which were associated with most measured soil properties shown by DistLM tests (Table S3).

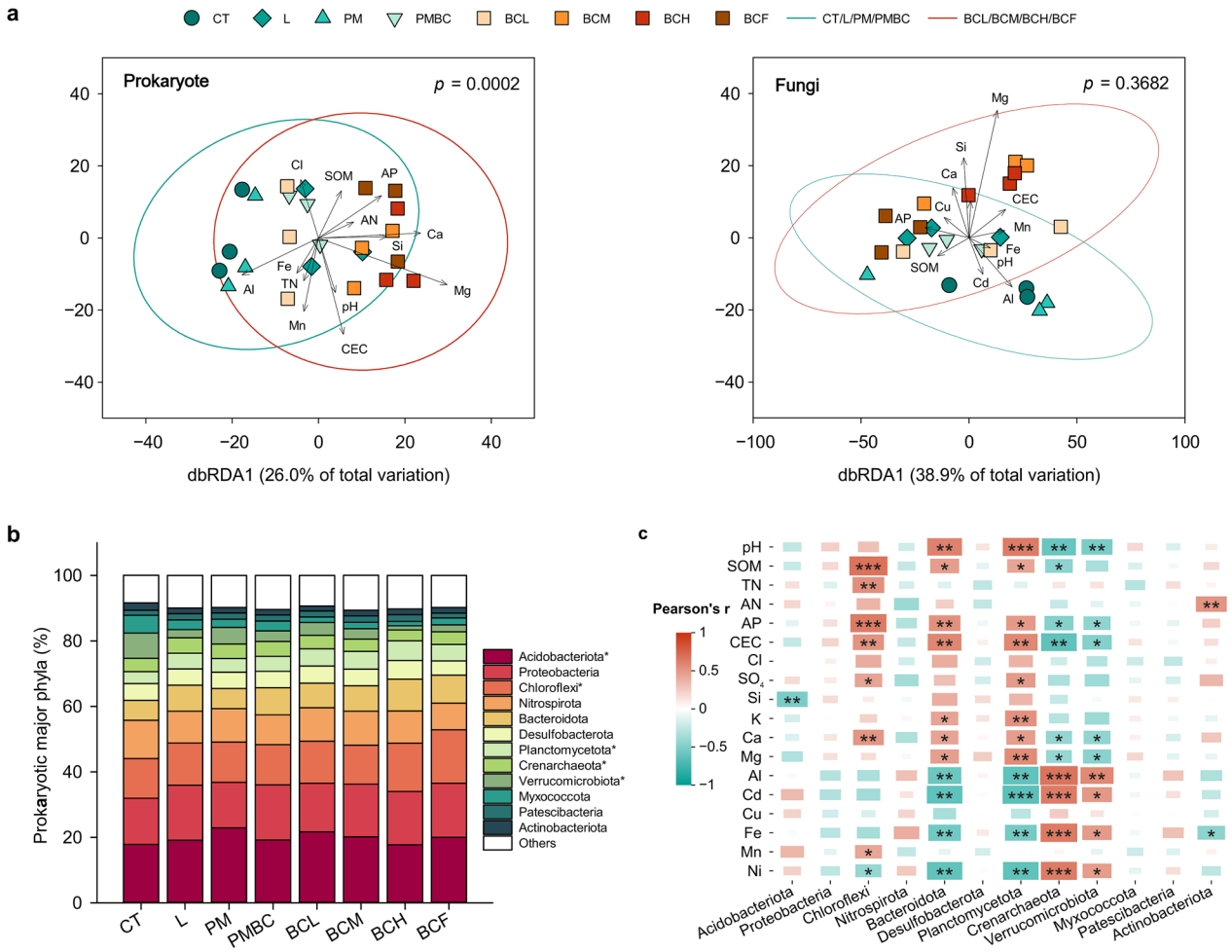

Fig. 2 **a** Distance-based redundancy analysis (dbRDA) of soil prokaryotic and fungal communities associated with soil characteristics, **b** the relative abundance of prokaryotic major phyla, and **c** Pearson's correlation between prokaryotic major phyla and soil characteristics under control (CT), lime (L), manure (PM), biochar with manure (PMBC), biochar at low (BCL), medium (BCM) and high dose (BCH), and biochar at 5-fold dose only in the first year (BCF). The prediction ellipse indicates 95% confidence region. Vectors represent the explanatory variables of soil characteristics. The asterisk indicates statistically significant differences among soil amendment treatments ($p < 0.05$); Statistical significances of Pearson's correlations are represented as follows: $^{*}p < 0.05$, $^{**}p < 0.01$, $^{***}p < 0.001$

Major prokaryotic phyla included Acidobacteriota (20%), Proteobacteria (16%), Chloroflexi (13%), and Nitrospirota (10%) (Fig. 2b). Compared to the control, PM and BCL amendments significantly enriched Acidobacteriota and increased the relative abundance of its class Vicinamibacteria by 25% ($p < 0.05$) (Fig. S3a). The BCF amendment enriched Chloroflexi, and the abundance of its class Anaerolineae was 35% greater than other treatments except BCH ($p < 0.05$) (Fig. S3a). In addition, the addition of biochar (BCL, BCM, BCH, and BCF) increased the abundance of Planctomycetota by 49% as well as its genera *Pirellula* and *Gemmata* ($p < 0.05$) (Fig. S3c). In contrast, the L, PMBC, BCM, BCH, and BCF amendments significantly suppressed Crenarchaeota by an average of 68% ($p < 0.05$), as well as its genera Candidatus *Nitrosotalea* and BSV13 (Fig. S3c). All the amendments lowered the relative abundance of Verrucomicrobiota by an average of 59% ($p < 0.05$), especially its genera Candidatus *Omnitrophus*, and ADurb. Bin063-1 (Fig. S3c). The abundances of Crenarchaeota and Verrucomicrobiota as well as the class Vicinamibacteria showed positive relationships to the concentrations of most metal ions but negative associations with soil basic properties and nutrient availability, while those of Chloroflexi (its class Anaerolineae) and Planctomycetota displayed the opposite trends (Fig. 2c, S3b). In comparison, the fungal composition exhibited no discernible differentiation and limited association with soil properties across the treatments (Fig. S4a, S4b).

All soil amendments except PM significantly increased the prokaryotic NRI compared to the control (Fig. S5). Moreover, the biochar treatments (BCL, BCM, BCH, and BCF) had significantly greater prokaryotic betaNRI than the other treatments. However, the co-occurrence networks did not show significant difference between the two above-mentioned groups of treatments in either prokaryotic or fungal communities (Fig. S6).

3.3 Metagenomic functions: biochar reshapes metabolic potential

The β-diversity of both metagenomic taxonomy ($p = 0.0066$) and function ($p = 0.0032$) significantly differed among the treatments (Fig. 3a). In particular, pairwise comparisons revealed marked differences in both metagenomic taxonomy and function between BCH and BCF relative to the control ($p < 0.05$) with biochar treatments associated positively with exchangeable Mg and Ca but negatively with bioavailable Al (Table S4). Similar to prokaryotic community, within metagenomic taxonomy, Chloroflexi exhibited a 7% increase in the BCH and BCF treatments, but an 8% decrease in the PM and PMBC treatments compared to the control ($p < 0.05$, Fig. S7a). Moreover, Verrucomicrobiota, especially its genera Candidatus Udaeobacter (Fig. S8), showed a broad decrease across all soil amendments and had negative relationships with soil basic properties and nutrient availability but positive associations with the bioavailability of most metals, while Bacteroidota and its genera *Flavobacterium* displayed an opposite trend ($p < 0.05$, Fig. S7b).

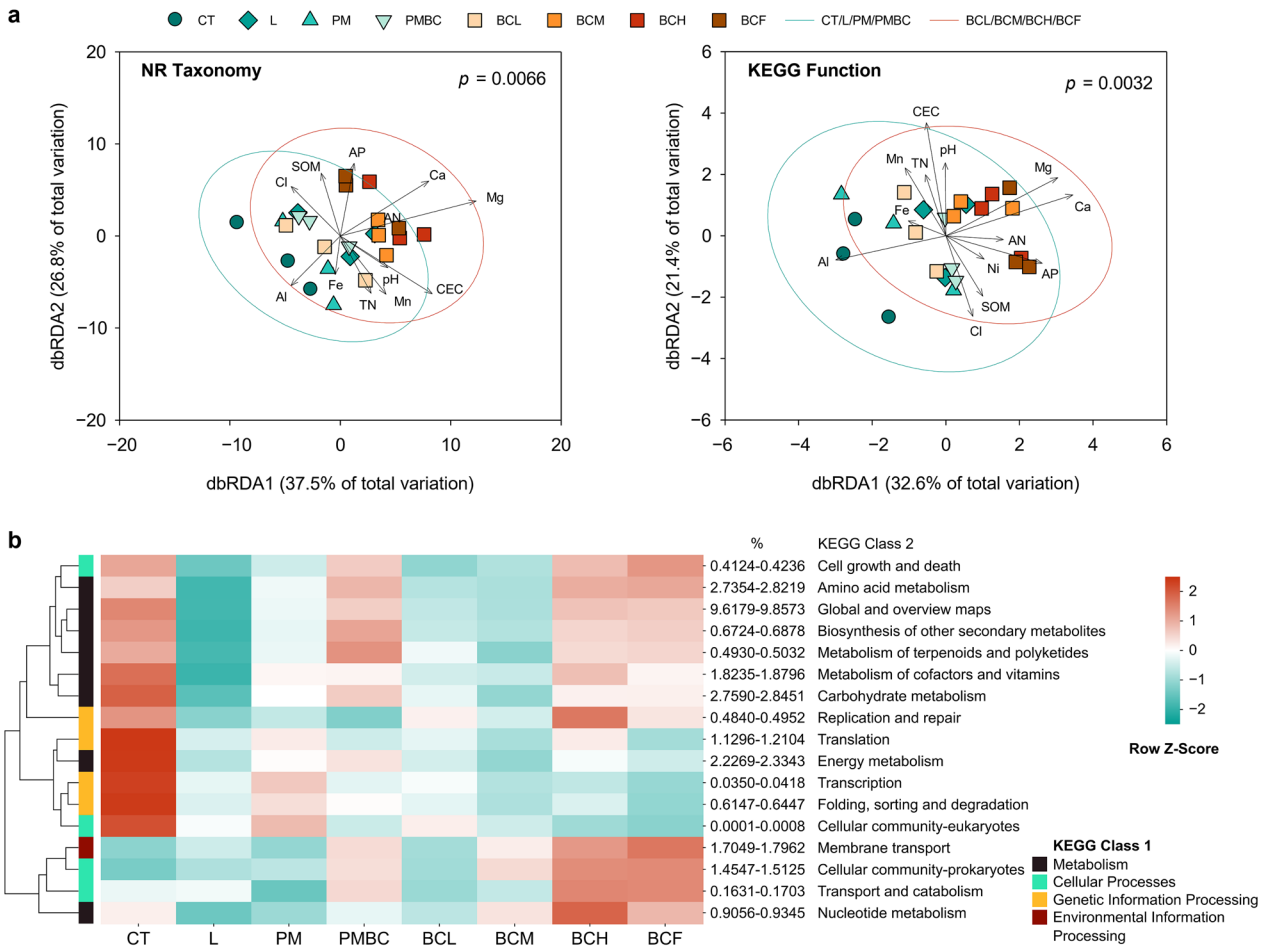

Fig. 3 **a** Distance-based redundancy analysis (dbRDA) of soil metagenomic taxa and functional categories annotated in National Center for Biotechnology Information (NCBI) Non-Redundant (NR) taxonomy database and Kyoto Encyclopedia of Genes and Genomes (KEGG) function database, respectively; **b** Heatmaps showing the relative abundance of soil metagenomic major functional categories annotated in KEGG at class 2 that significantly differ under control (CT), lime (L), manure (PM), biochar with manure (PMBC), biochar at low (BCL), medium (BCM) and high dose (BCH), and biochar at 5-fold dose only in the first year (BCF). The prediction ellipse in dbRDA indicates 95% confidence region. Vectors represent the explanatory variables of soil characteristics

For metagenomic functions, genes related to Genetic information processing, such as Translation, Transcription, Folding, sorting, and degradation, and Energy metabolism displayed an overall reduction following five-year soil amendments, which were positively associated with bioavailable metals ($p < 0.05$, Fig. 3b, S9). However, the BCH and BCF treatments significantly increased the relative abundance of Membrane Transport and Cellular Community (Prokaryotes) by 4–5% compared to the control, which were positively related to soil basic properties and nutrients but negatively associated with soil metal ions (Fig. S9). These treatments also enhanced that of Transport and catabolism, and Nucleotide metabolism by 2–3% in comparison with PM and L ($p < 0.05$, Fig. 3b). Moreover, liming decreased functional categories within metabolism, such as Amino acid, Carbohydrate, Terpenoids and polyketides, Cofactors and vitamins, and Biosynthesis of other secondary metabolites by 2–3% ($p < 0.05$).

At KEGG Class 3, high levels of biochar addition (BCH and BCF) significantly increased metabolic functions of Phenylalanine, Histidine, beta-Alanine, and D-Amino acid as well as ABC transporters and Quorum sensing compared to the control, and enhanced biosynthesis of Monobactam and Peptidoglycan as well as metabolisms of Purine, Pyrimidine, Fructose and mannose, Nicotinate and nicotinamide, Glycine, serine and threonine in comparison with the L treatment ($p < 0.05$, Fig. 4). In addition, BCH and BCF amendments lowered Photosynthesis, Pentose phosphate pathway, Starch and sucrose metabolism, while L, BCM, and BCF decreased Carbon and Methane metabolisms, Oxidative phosphorylation, and Citrate cycle ($p < 0.05$). The lime addition further decreased the relative abundance of genes related to biosynthesis of amino acids, arginine, cofactors, secondary metabolites as well as Metabolic pathways and Microbial metabolism in diverse environments ($p < 0.05$).

Metagenomic genes related to carbohydrate-active enzymes (CAZy genes) showed more significant segregation (Fig. 5a, $p < 0.0001$) between the control and amendment treatments than KEGG functions ($p = 0.0032$). In particular, biochar treatments (BCL, BCM, BCH, and BCF) were separated from control, and showed positive relationships with exchangeable Ca, Mg, and P availability but negative association with bioavailable Al and Fe (Table S5, $p < 0.05$). Consistent with the significant decrease of Carbohydrate metabolism found in KEGG functions, all amendments considerably decreased the relative abundance of CAZy genes compared to the control ($p < 0.05$, Fig. 5a). Specifically, the amendments significantly decreased the abundance of Glycoside Hydrolases (GHs), which positively correlated with the bioavailability of metal ions (Fig. S10a), with the largest decrease (average 6%) in the BCL, BCM, BCH, and BCF treatments (Fig. 5b, Fig. S11, $p < 0.05$). Conversely, BCH and BCF treatments increased the abundance of genes related to Auxiliary Activities (AAs) and Polysaccharide Lyases (PLs) by 8–9% compared to CT and PM (Fig. 5b, Fig. S11, $p < 0.05$), which showed positive correlations with basic soil properties and nutrient availability (Fig. S10a).

3.4 Soil virome: viral community responses and host interactions

Due to the significant influence of PM and BCH on soil microbiomes, metagenomics, and metabolomics, soil metaviromics were sequenced to further clarify and validate their effects on soil viral community and its potential bacterial hosts. Soil amendments had significant effects on soil metaviromic RPKM (Fig. 6a, $p = 0.0070$), with the BCH treatment positively associated with soil exchangeable Mg (Table S6). Specifically, in comparison with CT and/or PM, the BCH treatment enriched Algavirales, Crassvirales, and Imitervirales at the order level as well as Suoliviridae, Peduoviridae, and Phycodnaviridae at the family level (Fig. 6b, $p < 0.05$). Moreover, Cremevirales at the order level, Inoviridae and Zobellviridae at the family level exhibited greater decreases in both PM and BCH than CT ($p < 0.05$). Although the community structure of predicted bacterial hosts generally showed no significant difference between CT and amendments (Fig. 6a, $p = 0.0570$), certain taxa at the genus level, such as *Corynebacterium*, Candidatus *Hamiltonella*, and *Mannheimia*, significantly differed among treatments (Fig. 6c).

3.5 Metabolomic profiles: biochar-induced shifts in secondary metabolites

Microbial community characteristics and metabolomic profiles showed significant variations following the addition of soil amendments, especially BCH and BCF, that were positively related to soil exchangeable Ca, Mg, and N availability (Fig. 5a, Table S5, $p < 0.0001$). Generally, manure addition (PM and PMBC) increased metabolites belonging to Polyketides by 23% ($p < 0.05$, Fig. 5c), which were positively related to available N but negatively associated with Si (Fig. S10b).

Specifically, the BCF addition increased metabolites of lipids and lipid-like molecules, such as 3,6-dioxo-5alpha-cholan-24-oic acid, 7-ketolithocholic acid, apocholic acid, beta-amyrenonol, dehydrolithocholic acid, retinoic acid, and pomolic acid, as well as terpenoids, such as alisol B 23-acetate, elemadienonic acid, galdosol, and phytanic acid, but lowered benzoic acid, capric acid, eplerenone, lazabemide, piperonylic acid, smyrindioloside, tetradecylamine, trifolirhizin, and wogonoside

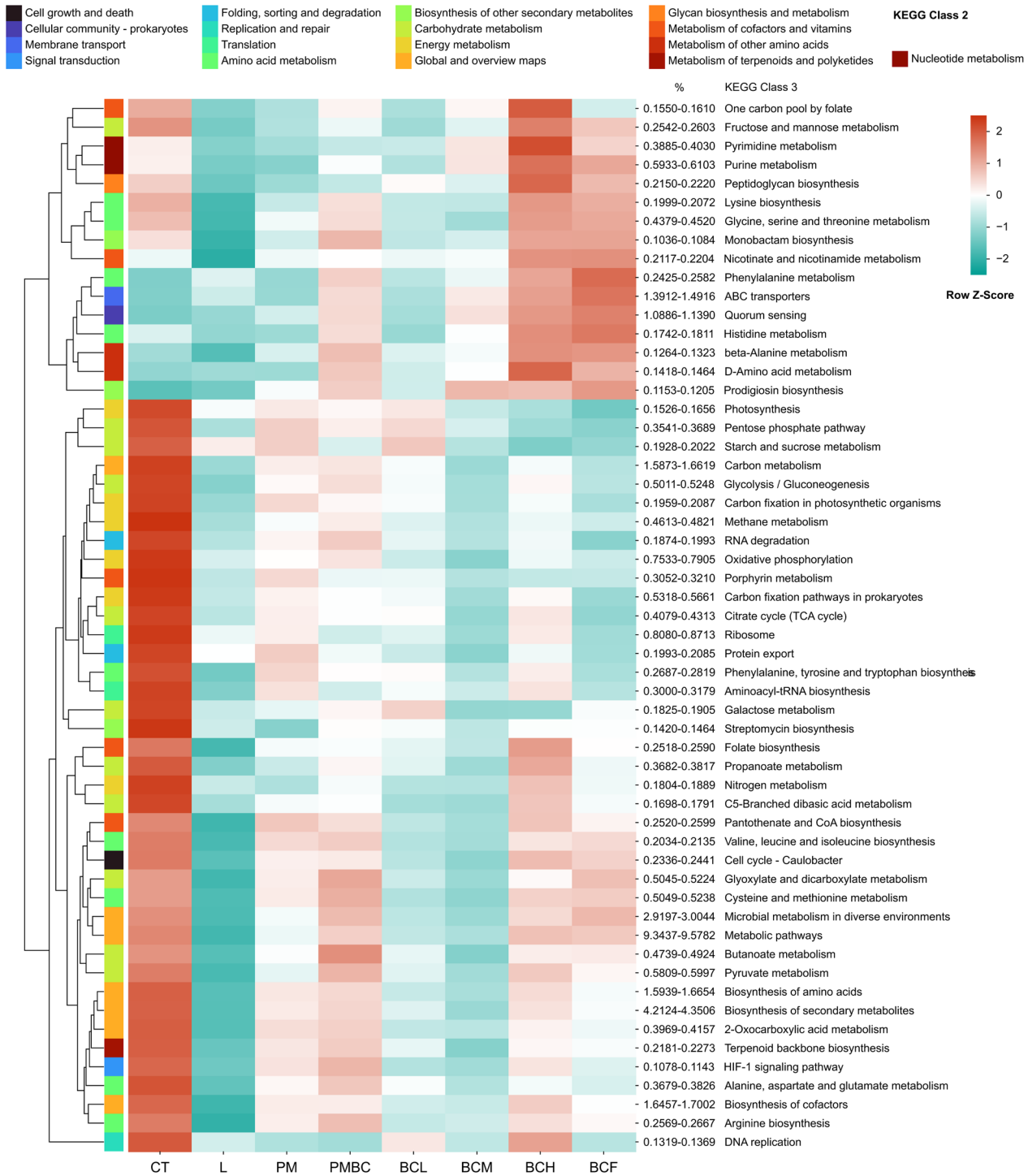

Fig. 4 Heatmaps showing the relative abundance of soil metagenomic functional categories annotated in KEGG function database at class 3 that significantly differ under control (CT), lime (L), manure (PM), biochar with manure (PMBC), biochar at low (BCL), medium (BCM) and high dose (BCH), and biochar at 5-fold dose only in the first year (BCF)

(Fig. 7, $p < 0.05$). Meanwhile, the BCH addition significantly increased sarcosine ethyl ester and hexamethylquercetagetin as well as organoheterocyclic compounds of 2-mercaptomethylbenzimidazole, 5-(chloromethyl)-1*H*-tetraazole, and 10-methylacridone ($p < 0.05$). In addition, the PM and PMBC treatments significantly

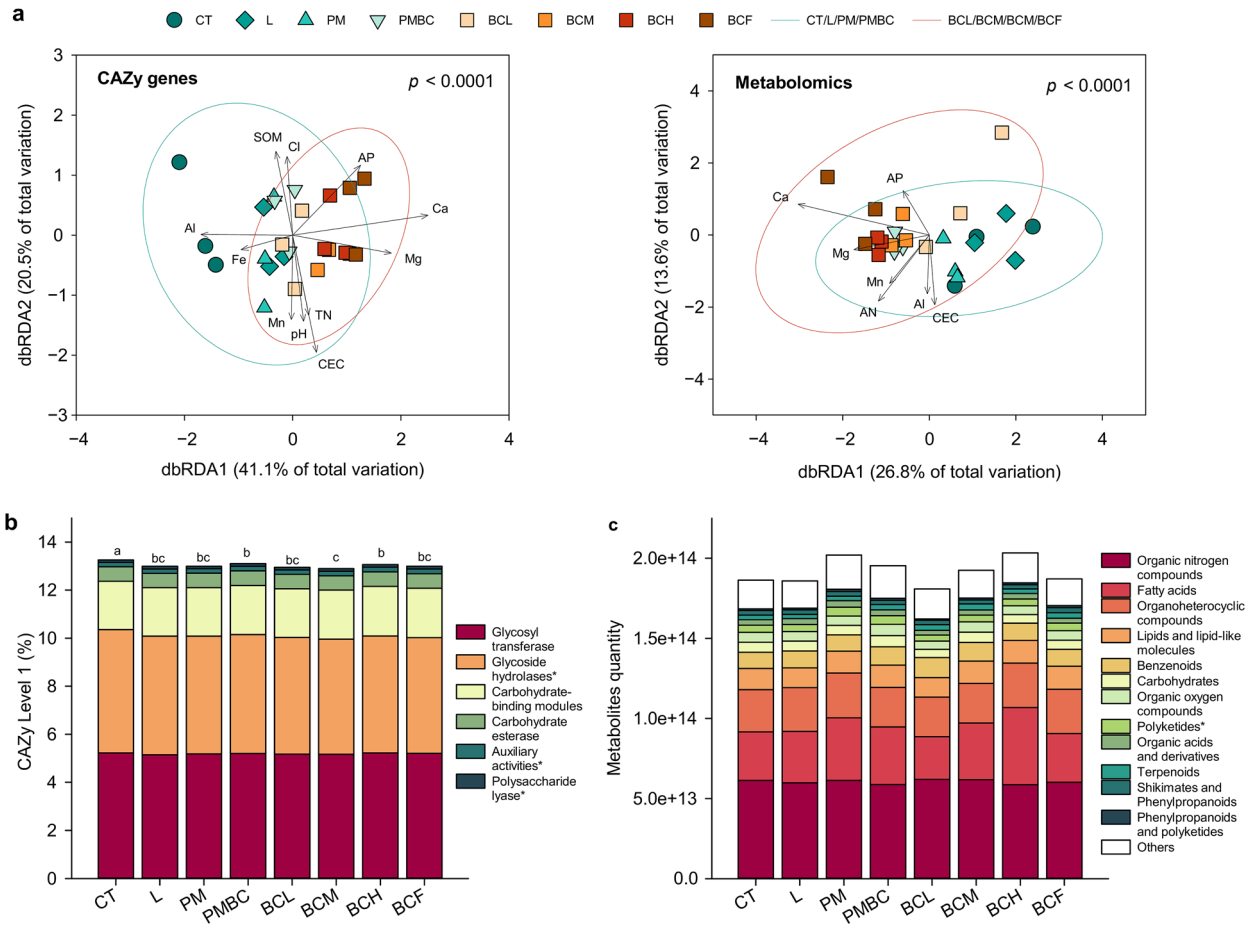

Fig. 5 **a** Distance-based redundancy analysis (dbRDA) of soil metagenomic functional categories annotated in carbohydrate-active enzymes (CAZy genes) function database at family levels and soil metabolites; **b** The relative abundance of soil metagenomic functional categories annotated in CAZy function database at level 1; **c** The quantity of soil metabolites grouped by major super classes under control (CT), lime (L), manure (PM), biochar with manure (PMBC), biochar at low (BCL), medium (BCM) and high dose (BCH), and biochar at 5-fold dose only in the first year (BCF). The prediction ellipse indicates 95% confidence region. Vectors represent the explanatory variables of soil characteristics. The asterisk indicates statistically significant differences among soil amendment treatments ($p < 0.05$)

increased 4-thiophene-3-carbonitrile, beta-D-glucopyranoside, eriodictyol-7-(6-galloylglucoside), hexadecane-6-carboxylic acid, nonanamide compared to the biochar treatments (BCL, BCM, and BCH) ($p < 0.05$).

3.6 Structural equation model: linking chemistry, communities, and metabolism

The SEM observed a direct influence of both nutrient availability (standardized path coefficient = 0.61, $p < 0.001$) and metal ions (0.46, $p < 0.01$) on soil metabolomic profiles (Fig. 8). Moreover, soil bioavailable metals could indirectly affect soil metabolomics through prokaryotic (0.58, $p < 0.05$) or fungal diversity (−0.78, $p < 0.05$) followed by metagenomic taxonomy (0.43, $p < 0.001$). Meanwhile, both prokaryotic (−0.61, $p < 0.001$) and fungal diversity (0.32, $p < 0.01$) had direct relation to metagenomic function. On the other hand, carbohydrate-active function was also directly affected by nutrient availability (−0.32, $p < 0.05$), and metagenomic taxonomy (0.31, $p < 0.001$) and function (0.43, $p < 0.001$).

4 Discussion

Our central research question asked whether long-term biochar application outperforms traditional amendments by orchestrating restructuring of soil microbiomes and metabolic functions. Our results support this hypothesis through evidence of a coordinated mechanistic cascade: biochar-induced improvements in soil chemistry (raised pH, increased nutrient availability, reduced metal bioavailability) drive restructuring of prokaryotic and viral communities, which in turn reshape metagenomic functions and metabolite profiles toward pathways supporting nutrient acquisition and carbon stabilization (Fig. 8). The following sections examine each stage of this cascade

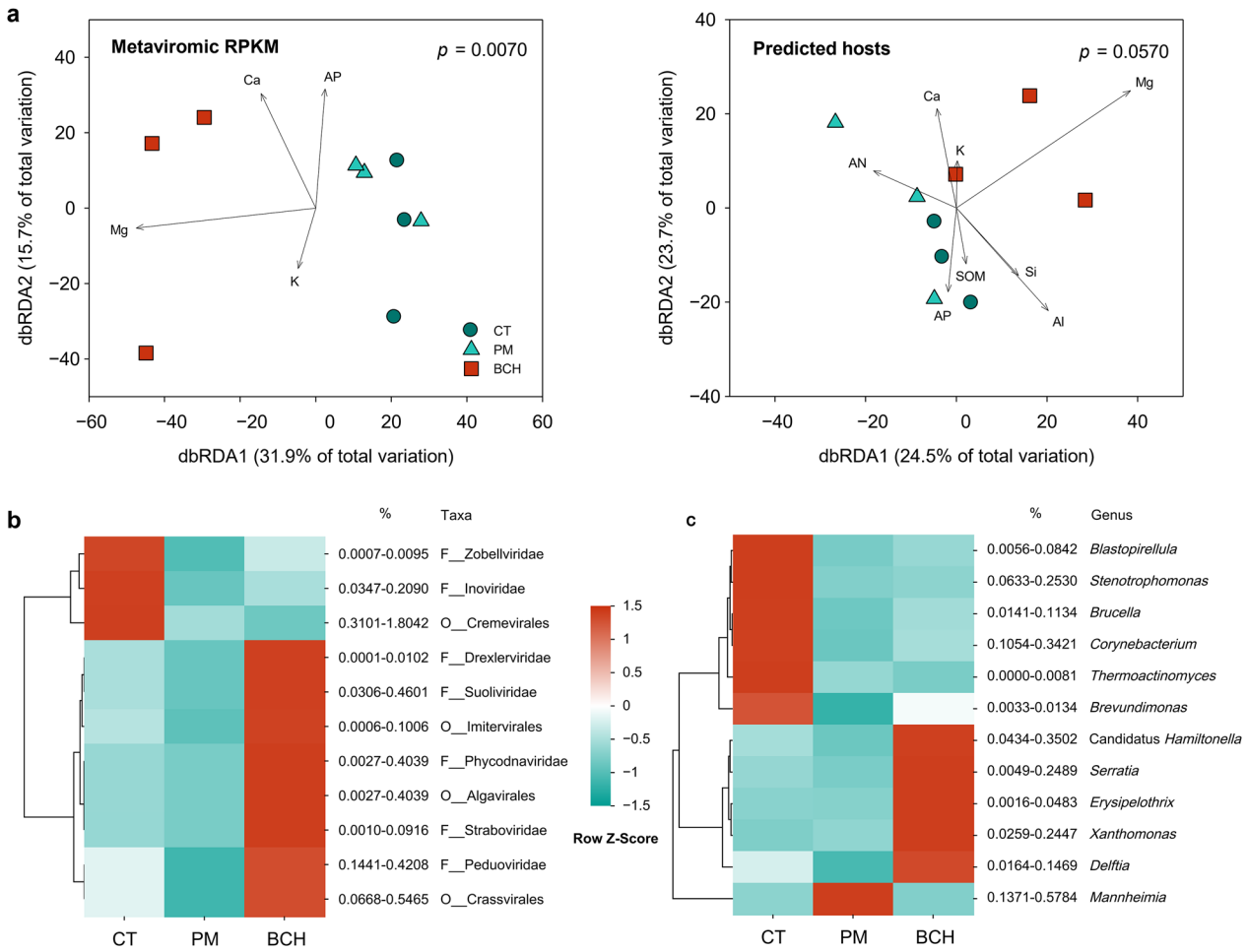

Fig. 6 **a** Distance-based redundancy analysis (dbRDA) of soil metaviromics calculated by the RPKM method (Reads Per Kilobase per Million mapped reads) and predicted bacterial hosts; **b** Heatmaps showing the relative abundance of major soil virus at order or family levels that significantly differ among the treatments; **c** Heatmaps showing the relative abundance of major predicted bacterial hosts at the genus level that significantly differ among amendment treatments. CT, control; PM, manure; BCH, biochar at relatively high dosages. Vectors represent the explanatory variables of soil characteristics

and its mechanisms, demonstrating how biochar's superiority over lime and swine manure emerges not from a single physicochemical property, but from its capacity to orchestrate sequential ecological changes that synergistically enhance soil health and crop productivity.

4.1 Biochar's chemical effects: foundation for ecological restructuring

Soil characteristics serve as key indicators of ecosystem functionality and health, directly reflecting the effectiveness of soil amendments in achieving sustainable agricultural intensification (Lehmann et al. 2020). Our results demonstrate that long-term field application of biochar not only mitigates soil acidification but also maintains nutrient availability and metal immobilization over multi-year timescales, properties that clearly distinguish biochar from traditional amendments (Fig. 1, Table S2).

In contrast, traditional amendments showed distinct limitations. Lime application did not significantly raise nutrient availability and led to a marked decrease in exchangeable K, likely due to competitive displacement by excess Ca^{2+} from calcium carbonate (Han et al. 2023). This limitation reflects its transient pH buffering capacity. Similarly, manure exhibited a limited capacity to regulate soil pH (Lauricella et al. 2020), because its organic matter-driven acidity neutralization cannot sustain the chemical environment required for consistent nutrient availability and metal immobilization. Moreover, swine manure not only failed to effectively reduce available Cd but may increase Cu accumulation through chelation processes (Ding et al. 2016), highlighting its constrained efficacy in mitigating metal bioavailability (Fig. 1a).

Biochar, especially at higher doses, demonstrated clear advantages over these conventional amendments. Its

Fig. 7 Heatmaps showing the quantity of soil metabolites that significantly differ control (CT), lime (L), manure (PM), biochar with manure (PMBC), biochar at low (BCL), medium (BCM) and high dose (BCH), and biochar at 5-fold dose only in the first year (BCF)

superior ability to improve basic soil properties, elevate nutrient concentrations, and lower bioavailability of metals can be attributed to a suite of unique physicochemical traits of high porosity, substantial surface area, inherent alkalinity, and elevated cation exchange capacity (Wang and Wang 2019). These properties collectively enhance soil structure, buffer pH, and improve nutrient retention. Furthermore, the diverse functional groups on biochar particle surfaces facilitate effective adsorption and immobilization of metal ions (Uchimiya et al. 2011). This metal immobilization persists over multi-year timescales, a capacity that coordinates with biochar's chemical

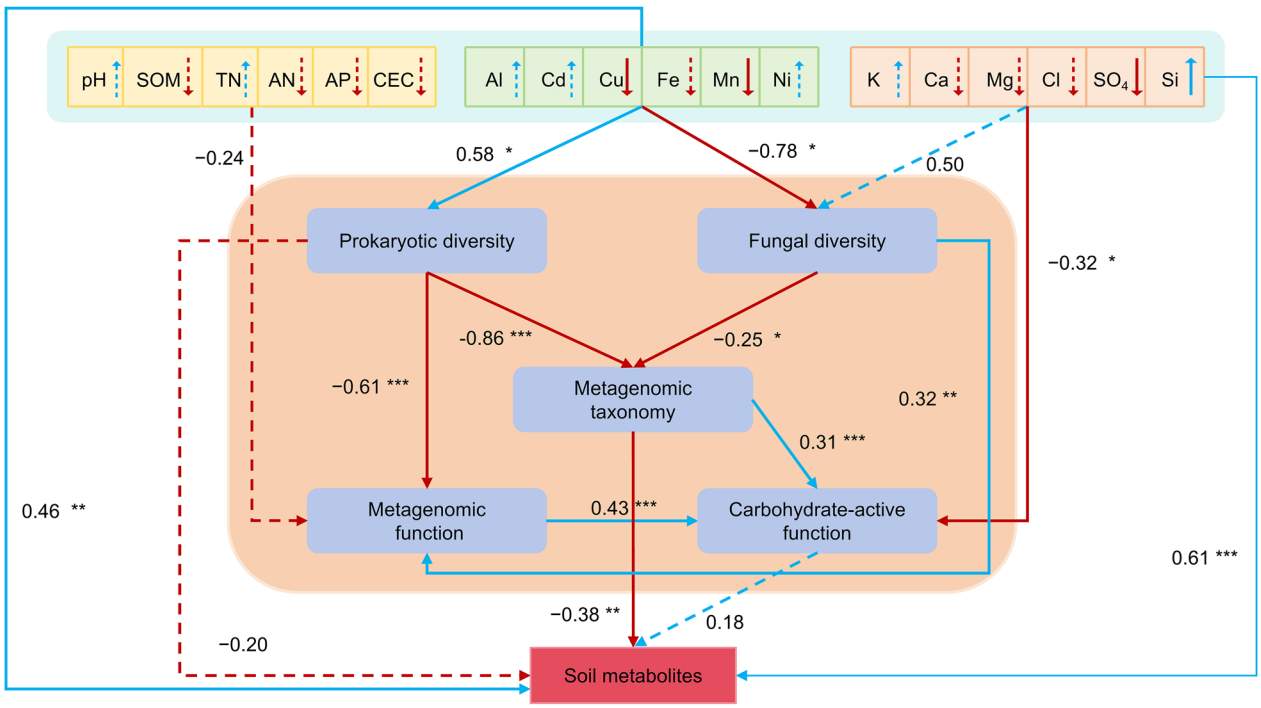

Fig. 8 Structural Equation Modeling (SEM) showing the effects of soil characteristics on soil microbial community and metagenomic functions as well as soil metabolites under different amendment treatments. The red and blue lines represent positive and negative pathways, respectively. Dashed lines indicate no significant correlation. The numbers near the arrows represent the standardized path coefficients; The asterisks indicate statistically significant correlations ($^{*}p < 0.05$, $^{**}p < 0.01$, $^{***}p < 0.001$)

improvement. This coordination of quality enhancement and contaminant control demonstrates that biochar addresses a core limitation of traditional amendments: the inability to simultaneously improve fertility and mitigate toxicity. For degraded agricultural systems, this dual capacity makes biochar strategically valuable for long-term soil restoration.

4.2 Community restructuring: how niochar reshapes prokaryotic and viral assemblages

Microorganisms are highly sensitive to soil changes (Fierer et al. 2021), among which bacteria often show greater sensitivity and diversity due to their direct metabolic reliance on external resources, whereas fungi maintain relative stability across varying environments by utilizing external organic matter. Our results also showed that prokaryotic diversity varied significantly across treatments, while fungal communities remained stable (Fig. 2a). Soils amended with high biochar doses (BCH, BCF) showed distinct separation in prokaryotic community structure from the control and other treatments (Figs. 2b, 3a), indicating a stronger ecological impact than traditional amendments.

Biochar addition significantly increased the relative abundance of Chloroflexi and Planctomycetota (Fig. 2b, S7a), extending observations by Zhang et al. (2021) with dose-dependent enrichment patterns under field conditions over five years. This long-term persistence reveals that biochar's capacity to enrich these groups represents a sustained ecological trajectory, not a transient response. The enrichment in Planctomycetota resulted from biochar-induced increases in soil porosity and moisture (El-Naggar et al. 2019). Over this five-year experiment, these improved microhabitats consistently supported copiotrophic taxa. Enrichment of its genera *Pirellula* and *Gemmata* (Fig. S3c), involved in organic C and N cycling (Dondjou et al. 2023), suggests that biochar facilitates processes like complex carbohydrate breakdown. Meanwhile, the close correlation between Chloroflexi enrichment and higher soil organic C (Fig. 2c) indicates enhanced organic matter turnover (Zheng et al. 2022) and hence soil fertility (Fierer et al. 2007). The class Anaerolineae within Chloroflexi also increased (Fig. S3a), likely due to anaerobic microsites created by water retention of biochar (Keiluweit et al. 2017).

In contrast, biochar suppressed acid-tolerant taxa, such as Crenarchaeota and its genera Candidatus *Nitrosotalea*

and BSV13, Verrucomicrobiota and its genera Candidatus *Omnitrophus*, Candidatus *Udaeobacter*, and ADurb. Bin063-1 (Fig. S3c), consistent with soil pH elevation (Neira et al. 2022). Conversely, PM promoted acidophilic groups like Acidobacteriota and Vicinamibacteria (Fig. S3a), likely by supplying labile C (Fierer et al. 2007). Regarding community assembly, PM did not significantly affect the prokaryotic phylogenetic structure of NRI (Fig. S5), whereas biochar enhanced deterministic assembly, increasing phylogenetic consistency of |betaNRI| (Stegen et al. 2013).

Metaviromic analysis revealed that viral communities responded markedly to biochar, but not to manure, with BCH forming a distinct cluster that separated from CT and PM (Fig. 6a). This indicates that high-dose biochar uniquely restructures soil viral assemblages. The BCH enriched specific viral taxa, including Crassvirales (order), Suoliviridae and Peduoviridae (family). Increased phage abundance likely intensifies infection-lysis cycles, releasing intracellular nutrients such as N and P, and accelerating nutrient turnover (Wu et al. 2022). Conversely, BCH suppressed taxa such as Cremevirales, Zobellviridae, and Inoviridae, reflecting shifts in virus-virus and virus-host interactions that may suppress certain bacterial lineages (Santos-Medellin et al. 2021). Viruses also mediate C and nutrient dynamics (Wei et al. 2021). The observed compositional shifts suggest that biochar may alter substrate availability, reduce microbial reliance on labile C, and slow the decomposition of soil organic matter, thereby enhancing C stability (Zhou et al. 2023). Together, viral and prokaryotic community restructuring under biochar reveals a key mechanism that traditional amendments cannot replicate. By enriching both prokaryotic and viral communities toward nutrient-cycling phenotypes, biochar creates a more functionally integrated microbial network. This viral-prokaryotic restructuring represents a previously underappreciated pathway through which biochar sustains long-term soil fertility and ecosystem function. Traditional amendments such as lime and manure do not generate this coordinated viral-prokaryotic response, highlighting a distinct mechanistic advantage in how biochar operates.

4.3 Functional reorganization: biochar drives coordinated changes in microbial metabolism

Due to the widespread functional redundancy among soil microbial taxa, shifts in microbial functional potential and metabolite profiles serve as a precise indicator of soil health status (Louca et al. 2018). While prior research has documented that amendments alter microbial functioning (Hu et al. 2022), our multi-year field study reveals a specific mechanism in biochar. Biochar orchestrates a coordinated functional restructuring: reductions in genetic information processing coupled with elevations in membrane transport and nutrient-exchange pathways create a functionally streamlined microbiome optimized for nutrient acquisition and carbon retention. Following five years of biochar application, we observed a reduction in the relative abundance of genes linked to Genetic information processing and Energy metabolism (Fig. 3b). This pattern may reflect genomic streamlining, wherein microorganisms in improved, nutrient-rich soils allocate fewer resources to maintaining complex genetic and high-energy metabolic pathways, favoring instead growth and reproduction (Wang et al. 2024).

Notably, high biochar application rates significantly increased the abundance of genes associated with Membrane transport and cellular community (Fig. 3b), suggesting enhanced microbial interaction and nutrient exchange (Zhu et al. 2017). Biochar also elevated metabolic activities related to Transport and catabolism, and Nucleotide metabolism. These shifts likely result from the ability of biochar to improve soil properties and provide stable nutrient supply (Gao et al. 2021), thereby stimulating genes involved in cellular activity and metabolic function (Hossain et al. 2020). Furthermore, high biochar rates increased the abundance of genes involved in Amino acid metabolism, ABC transporters, Quorum sensing, and the synthesis of structural and genetic components (Fig. 4), processes critical for microbial communication, survival, and community complexity (Abisado et al. 2018). Therefore, these functional changes elucidate how biochar restructures microbial metabolism by optimizing resource use and enhancing key processes such as nutrient uptake and cellular communication. This reorganization drives the assembly of a soil microbiome with greater functional coordination and environmental resilience.

In stark contrast, lime (L) significantly lowered the abundance of genes involved in metabolizing amino acids, carbohydrates, terpenoids, polyketides, cofactors, and vitamins (Figs. 3b, 4). This functional suppression reveals lime's mechanistic limitation. Lime-induced inhibition of acid-adapted microbial enzymes and metabolic functions (Wong and Fang 2000), coupled with alterations to soil structure that restrict oxygen, water, and nutrient availability (Ferreira et al. 2019), directly disrupted key biochemical pathways essential for nutrient cycling and metabolite production. These functional losses limited soil health in the long term (Hartmann and Six 2023). This suppression contrasts sharply with

biochar's coordinated functional enhancement, demonstrating that the two amendments operate through different ecological mechanisms.

The CAZy genes are crucial for carbohydrate breakdown, modification, and synthesis, playing a key role in organic matter decomposition and nutrient cycling (Ren et al. 2021). Soil amendments often supply readily available nutrients, reducing microbial dependence on complex carbohydrate degradation, which may lead to significant CAZy gene variations (Zhong et al. 2018). Our study further showed that all the amendments declined the abundance of glycoside hydrolase (GH) genes (Fig. 5), indicating reduced breakdown of complex sugars. Notably, biochar treatments increased auxiliary activity (AA) and polysaccharide lyase (PL) genes. AAs include oxidoreductases that support lignocellulose conversion (Levasseur et al. 2013), while PLs cleave uronic acid-rich polysaccharides (Lombard et al. 2010), indicating biochar redirects carbohydrate processing toward distinct enzymatic pathways.

Soil metabolite profiling offers further insight into microbial functioning and ecosystem services (Withers et al. 2020). We found that BCH and BCF treatments induced pronounced shifts in metabolite profiles (Figs. 5, 6), consistent with the observations by Cui et al. (2024) and Liu et al. (2023) in other cropping systems. Specifically, lipids, lipid-like molecules, and terpenoids increased under BCH (Fig. 7), including alisol B 23-acetate and galdosol, which may support plant growth, pathogen defense, or microbial signaling (Tyc et al. 2017). Conversely, the decrease in benzoic acid suggests altered soil chemistry, possibly due to biochar adsorption, microbial restructuring, or anaerobic microsite formation (Singh et al. 2022). Increased organoheterocyclic compounds further imply enhanced pollutant detoxification and nutrient availability, reflecting improved habitat suitability and microbial activity (Palansooriya et al. 2019).

Treatments PM and PMBC elevated polyketides through abundant humic and phenolic compounds that stimulate transient microbial metabolism (Sun et al. 2024), including 4-thiophene-3-carbonitrile and β-D-glucopyranoside. In contrast, lime induced minimal metabolite changes, reflecting its functional suppression and inability to sustain chemical conditions supporting secondary metabolism (Hartmann and Six 2023). The metabolite data reveal a mechanistic distinction among amendments. Biochar orchestrates a sustained restructuring of the soil metabolome toward lipids and terpenoids that provide substrate for nutrient-cycling microbes and plant-protective compounds. This metabolomic restructuring is absent under lime and transient under manure. The restructuring represents the final stage of biochar's mechanistic cascade: soil chemistry drives community shifts, which enable functional changes, and subsequently reshape the metabolome. This integrated metabolomic response explains how biochar achieves superior long-term soil health outcomes compared to conventional amendments.

4.4 Integrating the cascade: mechanistic understanding of biochar's long-term superiority

Our investigation of mechanisms underlying biochar's superiority examines how soil chemistry changes propagate through biological systems. Biochar amendment improves soil porosity, water retention, and aggregate stability, creating diverse microhabitats that support microbial colonization and metabolic activity (Annabi et al. 2011). Simultaneously, biochar elevates soil pH and supplies essential nutrients, which buffer acidity and regulate microbial biochemistry (Dai et al. 2021). Our data demonstrate that these chemical improvements correlate tightly with shifts in microbial diversity, composition, and metabolic function (Figs. 2c, S7b, S9, S10). The correlation was consistent with established understanding that soil structure and chemistry directly influence microbial properties (Bai et al. 2020). Specifically, improved soil properties and nutrient levels correlated positively with beneficial microbial shifts, while bioavailable metals correlated negatively with these shifts, confirming the pivotal role of the soil chemical environment in driving microbial community assembly and function (Yuan et al. 2011).

Under biochar treatments, improved nutrient availability and suppression of bioavailable metals, particularly Al, mediated changes in microbial community composition and metabolic function (Figs. 2a, 3a, 5a, and 6a). The ionic mechanisms are revealing. Calcium stabilizes membranes, facilitates cellular signaling, and supports cell–cell interactions that enable community-level cooperation (Clapham 2007). Magnesium acts as a cofactor in nucleic acid and energy metabolism, fueling increased biosynthetic activity under biochar amendment (Pasternak et al. 2010). In contrast, high levels of bioavailable Al and Cd directly disrupt enzyme activity and cellular structures, suppressing microbial metabolism and viability (Karaca et al. 2010). These ionic shifts, demonstrated through SEM (Fig. 8), reveal how soil chemical changes translate into shifts in the soil metabolome. Microbial functionality serves as the key intermediary linking soil chemistry to metabolite profiles, enabling the integrated soil-microbe-metabolite response observed under biochar amendment.

This mechanistic understanding reveals how biochar's mechanism diverges from traditional amendments. The cascade operates through three sequential stages. First, biochar improves soil physicochemical properties: elevating pH, increasing nutrient availability, and suppressing bioavailable metals. Second, these chemical changes drive restructuring of both prokaryotic and viral communities toward assemblages enriched in nutrient-cycling taxa and phages that accelerate nutrient turnover. Third, the restructured microbial and viral communities reshape metagenomic function and soil metabolite profiles, enriching lipids and terpenoids that support plant growth and long-term carbon stabilization. Unlike lime, which transiently raises pH without sustaining biological restructuring, and unlike manure, which supplies transient carbon without orchestrating coordinated ecological change, biochar's superiority emerges from this integrated cascade. The cascade operates across soil chemistry, microbial ecology, and metabolic function as an interconnected whole. This integrated mechanism explains how biochar, unlike traditional amendments, sustains long-term enhancements in soil health and crop productivity. For degraded acidic agricultural systems globally, understanding this mechanistic cascade provides the scientific foundation for deploying biochar as an ecosystem restoration tool rather than a simple soil amendment. This perspective has profound implications for sustainable intensification of marginal lands and for global food security in the face of soil degradation and climate change.

5 Conclusions

This five-year field experiment demonstrates that high-dose biochar outperforms lime and swine manure in alleviating soil acidity and improving soil fertility in an acidic paddy soil. Biochar's superiority emerges from a mechanistic cascade that traditional amendments cannot replicate: improved soil chemistry drives restructuring of prokaryotic and viral communities, which reshape metagenomic functions and soil metabolite profiles. Unlike lime, which transiently raises pH without coordinating ecological change, and unlike manure, which supplies transient carbon without orchestrating sustained community shifts, biochar creates a tightly coordinated response across soil chemistry, microbiology, and metabolism. This integrated mechanism explains how biochar sustains long-term improvements in nutrient availability, metal immobilization, microbial function, and crop productivity. The findings provide mechanistic evidence that biochar operates as an ecosystem restoration tool rather than a simple soil amendment. For degraded acidic agricultural systems globally, this understanding establishes a scientific foundation for optimized biochar deployment to support sustainable soil restoration and agricultural resilience.

Supplementary Information

The online version contains supplementary material available at https://doi.org/10.1007/s42773-026-00598-9.

Supplementary Material 1.

Author contributions

Jun Meng: Writing-review & editing, Methodology, Conceptualization, Investigation, Formal analysis, Funding acquisition. Zhonghua Cui: Validation, Software, Data curation. Zhangtao Li: Formal analysis, Data curation. Jiaxin Li: Writing-review & editing, Writing-original draft, Visualization, Software. Minjun Hu: Resources, Conceptualization. Jun Xu: Resources, Conceptualization. Zhiyuan Yao: Methodology, Investigation, Formal analysis. Caixian Tang: Writing-review & editing, Resources, Conceptualization. Dong Yang: Methodology, Funding acquisition, Conceptualization. Alexandru Ozunu: Resources, Conceptualization. Shengdao Shan: Methodology, Resources, Conceptualization. Huaihai Chen: Writing-review & editing, Writing-original draft, Visualization, Validation, Methodology, Investigation, Funding acquisition.

Funding

This work was financially funded by the National Natural Science Foundation of China (42277282, 42207018), the Public Welfare Technology Application Research Project of Zhejiang Province, China (LGF21D010002), Zhejiang Province "Three Rural Nine Strategies" Science and Technology Cooperation Program (2024SNJF068), Shenzhen Science and Technology Program (JCYJ20250604174440054, JCYJ20220530150201003), and Basic and Applied Basic Research Foundation of Guangdong Province (2022A1515010861).

Data availability

The sequencing raw data are deposited in the NCBI Short Read Archive database under accession numbers PRJNA1102840.

Declarations

Competing interests

There are no competing interests involved in the article.

Author details

[1]School of Environmental and Natural Resources, Zhejiang University of Science and Technology, Hangzhou 310023, China. [2]State Key Laboratory of Biocontrol, School of Ecology, Shenzhen Campus of Sun Yat-sen University, Shenzhen 518107, China. [3]Agricultural Technology Extension Center, Agriculture and Rural Affairs Bureau of Fuyang District, Hangzhou 311499, China. [4]Institute of Hydraulic and Ocean Engineering, School of Civil and Environmental Engineering and Geography Science, Ningbo University, Ningbo 315211, China. [5]Department of Ecological, Plant and Animal Sciences, La Trobe Institute for Sustainable Agriculture and Food, La Trobe University, Bundoora, VIC 3086, Australia. [6]Quality and Fertilizer Administration Bureau of Zhejiang Province, Hangzhou 310020, China. [7]Faculty of Environmental Science and Engineering, Babeș-Bolyai University, 30 Fântânele St., 400294 Cluj-Napoca, Romania.

Received: 5 May 2025 Revised: 11 February 2026 Accepted: 25 February 2026
Published online: 25 March 2026

References

Abarenkov K, Nilsson RH, Larsson K-H, Taylor AFS, May TW, Frøslev TG, Pawlowska J, Lindahl B, Põldmaa K, Truong C, Vu D, Hosoya T, Niskanen T, Piirmann T, Ivanov F, Zirk A, Peterson M, Cheeke TE, Ishigami Y, Jansson AT, Jeppesen TS, Kristiansson E, Mikryukov V, Miller JT, Oono R, Ossandon FJ, Paupério J, Saar I, Schigel D, Suija A, Tedersoo L, Kõljalg U (2024) The

UNITE database for molecular identification and taxonomic communication of fungi and other eukaryotes: sequences, taxa and classifications reconsidered. Nucleic Acids Res 52(D1):D791–D797. https://doi.org/10.1093/nar/gkad1039
Abisado RG, Benomar S, Klaus JR, Dandekar AA, Chandler JR (2018) Bacterial quorum sensing and microbial community interactions. Mbio 9(3):10.1128/mbio.02331-17. https://doi.org/10.1128/mbio.02331-17
Alseekh S, Aharoni A, Brotman Y, Contrepois K, D'Auria J, Ewald J, Ewald JC, Fraser PD, Giavalisco P, Hall RD, Heinemann M, Link H, Luo J, Neumann S, Nielsen J, Perez de Souza L, Saito K, Sauer U, Schroeder FC, Schuster S, Siuzdak G, Skirycz A, Sumner LW, Snyder MP, Tang H, Tohge T, Wang Y, Wen W, Wu S, Xu G, Zamboni N, Fernie AR (2021) Mass spectrometry-based metabolomics: a guide for annotation, quantification and best reporting practices. Nat Methods 18(7):747–756. https://doi.org/10.1038/s41592-021-01197-1
Altschul SF, Gish W, Miller W, Myers EW, Lipman DJ (1990) Basic local alignment search tool. J Mol Biol 215(3):403–410. https://doi.org/10.1016/S0022-2836(05)80360-2
Annabi M, Le Bissonnais Y, Le Villio-Poitrenaud M, Houot S (2011) Improvement of soil aggregate stability by repeated applications of organic amendments to a cultivated silty loam soil. Agric Ecosyst Environ 144(1):382–389. https://doi.org/10.1016/j.agee.2011.07.005
Bai N, Zhang H, Zhou S, Sun H, Zhao Y, Zheng X, Li S, Zhang J, Lv W (2020) Long-term effects of straw return and straw-derived biochar amendment on bacterial communities in soil aggregates. Sci Rep 10(1):7891. https://doi.org/10.1038/s41598-020-64857-w
Biddle JF, Fitz-Gibbon S, Schuster SC, Brenchley JE, House CH (2008) Metagenomic signatures of the Peru Margin subseafloor biosphere show a genetically distinct environment. Proc Natl Acad Sci USA 105(30):10583–10588. https://doi.org/10.1073/pnas.0709942105
Biederman LA, Harpole WS (2013) Biochar and its effects on plant productivity and nutrient cycling: a meta-analysis. GCB Bioenergy 5(2):202–214. https://doi.org/10.1111/gcbb.12037
Buchfink B, Xie C, Huson DH (2015) Fast and sensitive protein alignment using DIAMOND. Nat Methods 12(1):59–60. https://doi.org/10.1038/nmeth.3176
Bunemann EK, Bongiorno G, Bai Z, Creamer RE, De Deyn G, de Goe R, Fleskens L, Geissen V, Kuyper TW, Mader P, Pulleman M, Sukkel W, van Groenigen JW, Brussaard L (2018) Soil quality-a critical review. Soil Biol Biochem 120:105–125. https://doi.org/10.1016/j.soilbio2018.01.030
Callahan BJ, McMurdie PJ, Rosen MJ, Han AW, Johnson AJA, Holmes SP (2016) DADA2: High-resolution sample inference from Illumina amplicon data. Nat Methods 13(7):581–583. https://doi.org/10.1038/nmeth.3869
Chen S (2023) Ultrafast one-pass FASTQ data preprocessing, quality control, and deduplication using fastp. iMeta 2(2):e107. https://doi.org/10.1002/imt2.107
Chen W, Meng J, Han X, Lan Y, Zhang W (2019) Past, present, and future of biochar. Biochar 1(1):75–87. https://doi.org/10.1007/s42773-019-00008-3
Chen D, Wang X, Carrión VJ, Yin S, Yue Z, Liao Y, Dong Y, Li X (2022) Acidic amelioration of soil amendments improves soil health by impacting rhizosphere microbial assemblies. Soil Biol Biochem 167:108599. https://doi.org/10.1016/j.soilbio.2022.108599
Clapham DE (2007) Calcium signaling. Cell 131(6):1047–1058. https://doi.org/10.1016/j.cell.2007.11.028
Cui X, Yuan J, Yang X, Wei C, Bi Y, Sun Q, Meng J, Han X (2024) Biochar application alters soil metabolites and nitrogen cycle-related microorganisms in a soybean continuous cropping system. Sci Total Environ 917:170522. https://doi.org/10.1016/j.scitotenv.2024.170522
Dai Z, Xiong X, Zhu H, Xu H, Leng P, Li J, Tang C, Xu J (2021) Association of biochar properties with changes in soil bacterial, fungal and fauna communities and nutrient cycling processes. Biochar 3(3):239–254. https://doi.org/10.1007/s42773-021-00099-x
Ding Y, Liu Y, Liu S, Li Z, Tan X, Huang X, Zeng G, Zhou L, Zheng B (2016) Biochar to improve soil fertility. A review. Agron Sustain Dev 36(2):36. https://doi.org/10.1007/s13593-016-0372-z
Dixon P (2003) VEGAN, a package of R functions for community ecology. J Veg Sci 14(6):927–930. https://doi.org/10.1111/j.1654-1103.2003.tb02228.x
Dodor DE, Tabatabai MA (2019) A simple alkaline hydrolysis method for estimating nitrogen mineralization potential of soils. West Afr J Appl Ecol 27(2):16–31. https://doi.org/10.4314/wajae.v27i2
Dondjou DT, Diedhiou AG, Mbodj D, Mofini M-T, Pignoly S, Ndiaye C, Diedhiou I, Assigbetse K, Manneh B, Laplaze L, Kane A (2023) Rice developmental stages modulate rhizosphere bacteria and archaea co-occurrence and sensitivity to long-term inorganic fertilization in a West African Sahelian agro-ecosystem. Environ Microbiome 18(1):42. https://doi.org/10.1186/s40793-023-00500-1
Edgar RC (2010) Search and clustering orders of magnitude faster than BLAST. Bioinformatics 26(19):2460–2461. https://doi.org/10.1093/bioinformatics/btq461
El-Naggar A, Lee SS, Rinklebe J, Farooq M, Song H, Sarmah AK, Zimmerman AR, Ahmad M, Shaheen SM, Ok YS (2019) Biochar application to low fertility soils: a review of current status, and future prospects. Geoderma 337:536–554. https://doi.org/10.1016/j.geoderma.2018.09.034
Ferreira TR, Pires LF, Wildenschild D, Brinatti AM, Borges JAR, Auler AC, dos Reis AMH (2019) Lime application effects on soil aggregate properties: use of the mean weight diameter and synchrotron-based X-ray μCT techniques. Geoderma 338:585–596. https://doi.org/10.1016/j.geoderma.2018.10.035
Fierer N, Bradford MA, Jackson RB (2007) Toward an ecological classification of soil bacteria. Ecology 88(6):1354–1364. https://doi.org/10.1890/05-1839
Fierer N, Wood SA, de Bueno Mesquita CP (2021) How microbes can, and cannot, be used to assess soil health. Soil Biol Biochem 153:108111. https://doi.org/10.1016/j.soilbio2020.108111
Frimpong KA, Owusu S, Darko RO, Hanyabui E, Abbey ANA, Tetteh DA (2025) Effect of biochar application rates on soil properties and growth of amaranthus caudatus. Discover Agriculture 3(1):1–17. https://doi.org/10.1007/s44279-025-00172-0
Fu Y, de Jonge LW, Moldrup P, Paradelo M, Arthur E (2022) Improvements in soil physical properties after long-term manure addition depend on soil and crop type. Geoderma 425:116062. https://doi.org/10.1016/j.geoderma.2022.116062
Fu Q, Qiu YB, Zhao J, Li J, Xie S, Liao Q, Fu X, Huang Y, Yao Z, Dai Z, Qiu YP, Yang Y, Li F, Chen H (2024) Monotonic trends of soil microbiomes, metagenomic and metabolomic functioning across ecosystems along water gradients in the Altai region, northwestern China. Sci Total Environ 912:169351. https://doi.org/10.1016/j.scitotenv.2023.169351
Gao M, Yang J, Liu C, Gu B, Han M, Li J, Li N, Liu N, An N, Dai J, Liu X, Han X (2021) Effects of long-term biochar and biochar-based fertilizer application on brown earth soil bacterial communities. Agric Ecosyst Environ 309:107285. https://doi.org/10.1016/j.agee.2020.107285
Gardes M, Bruns TD (1993) ITS primers with enhanced specificity for basidiomycetes—application to the identification of mycorrhizae and rusts. Mol Ecol 2(2):113–118. https://doi.org/10.1111/j.1365-294X.1993.tb00005.x
Guo J, Bolduc B, Zayed AA, Varsani A, Dominguez-Huerta G, Delmont TO, Pratama AA, Gazitúa MC, Vik D, Sullivan MB, Roux S (2021) VirSorter2: a multi-classifier, expert-guided approach to detect diverse DNA and RNA viruses. Microbiome 9(1):37. https://doi.org/10.1186/s40168-020-00990-y
Han T, Li D, Liu K, Huang J, Zhang L, Liu S, Shah A, Liu L, Feng G, Zhang H (2023) Soil potassium regulation by initial K level and acidification degree when subjected to liming: a meta-analysis and long-term field experiment. CATENA 232:107408. https://doi.org/10.1016/j.catena.2023.107408
Hartmann M, Six J (2023) Soil structure and microbiome functions in agroecosystems. Nat Rev Earth Env 4(1):4–18. https://doi.org/10.1038/s43017-022-00366-w
Hossain MZ, Bahar MM, Sarkar B, Donne SW, Ok YS, Palansooriya KN, Kirkham MB, Chowdhury S, Bolan N (2020) Biochar and its importance on nutrient dynamics in soil and plant. Biochar 2(4):379–420. https://doi.org/10.1007/s42773-020-00065-z
Hu M, Xiang Y, Lu J (2016a) Effects of lime application rates on soil acidity and barley seeding growth in acidic soils. Sci Agric Sin 49(20):3896–3903. https://doi.org/10.3864/j.issn.0578-1752.2016.20.004
Hu Y, Cheng H, Tao S (2016b) The challenges and solutions for cadmium-contaminated rice in China: a critical review. Environ Int 92:515–532. https://doi.org/10.1016/j.envint.2016.04.042
Hu X, Gu H, Liu J, Wei D, Zhu P, Cui X, Zhou B, Chen X, Jin J, Liu X, Wang G (2022) Metagenomics reveals divergent functional profiles of soil carbon and nitrogen cycling under long-term addition of chemical and organic fertilizers in the black soil region. Geoderma 418:115846. https://doi.org/10.1016/j.geoderma.2022.115846
Huang Y, Shi W, Fu Q, Qiu YB, Zhao J, Li J, Lyu Q, Yang X, Xiong J, Wang W, Chang R, Yao Z, Dai Z, Qiu YP, Chen H (2023) Soil development following glacier retreat shapes metagenomic and metabolomic functioning

associated with asynchronous C and N accumulation. Sci Total Environ 892:164405. https://doi.org/10.1016/j.scitotenv.2023.164405
Hyatt D, Chen G-L, LoCascio PF, Land ML, Larimer FW, Hauser LJ (2010) Prodigal: prokaryotic gene recognition and translation initiation site identification. BMC Bioinformatics 11(1):119. https://doi.org/10.1186/1471-2105-11-119
Karaca A, Cetin SC, Turgay OC, Kizilkaya R (2010) Effects of heavy metals on soil enzyme activities. Soil heavy metals. Springer, Berlin, Heidelberg, pp 237–262. https://doi.org/10.1007/978-3-642-02436-8-11
Keiluweit M, Wanzek T, Kleber M, Nico P, Fendorf S (2017) Anaerobic microsites have an unaccounted role in soil carbon stabilization. Nat Commun 8:1771. https://doi.org/10.1038/s41467-017-01406-6
Kembel SW, Cowan PD, Helmus MR, Cornwell WK, Morlon H, Ackerly DD, Blomberg SP, Webb CO (2010) Picante: R tools for integrating phylogenies and ecology. Bioinformatics 26(11):1463–1464. https://doi.org/10.1093/bioinformatics/btq166
Kerner P, Struhs E, Mirkouei A, Aho K, Lohse KA, Dungan RS, You Y (2023) Microbial responses to biochar soil amendment and influential factors: a three-level meta-analysis. Environ Sci Technol 57(48):19838–19848. https://doi.org/10.1021/acs.est.3c04201
Kuzyakov Y, Mason-Jones K (2018) Viruses in soil: nano-scale undead drivers of microbial life, biogeochemical turnover and ecosystem functions. Soil Biol Biochem 127:305–317. https://doi.org/10.1016/j.soilbio.2018.09.032
Lauricella D, Butterly CR, Clark GJ, Sale PWG, Li G, Tang C (2020) Effectiveness of innovative organic amendments in acid soils depends on their ability to supply P and alleviate Al and Mn toxicity in plants. J Soil Sediment 20(11):3951–3962. https://doi.org/10.1007/s11368-020-02721-0
Lehmann J (2007) A handful of carbon. Nature 447(7141):143–144. https://doi.org/10.1038/447143a
Lehmann J, Bossio DA, Kögel-Knabner I, Rillig MC (2020) The concept and future prospects of soil health. Nat Rev Earth Environ 1(10):544–553. https://doi.org/10.1038/s43017-020-0080-8
Levasseur A, Drula E, Lombard V, Coutinho PM, Henrissat B (2013) Expansion of the enzymatic repertoire of the CAZy database to integrate auxiliary redox enzymes. Biotechnol Biofuels 6(1):41. https://doi.org/10.1186/1754-6834-6-41
Li D, Luo R, Liu C-M, Leung C-M, Ting H-F, Sadakane K, Yamashita H, Lam T-W (2016) MEGAHIT v1.0: a fast and scalable metagenome assembler driven by advanced methodologies and community practices. Methods 102:3–11. https://doi.org/10.1016/j.ymeth.2016.02.020
Li X-M, Chen Q-L, He C, Shi Q, Chen S-C, Reid BJ, Zhu Y-G, Sun G-X (2019) Organic carbon amendments affect the chemodiversity of soil dissolved organic matter and its associations with soil microbial communities. Environ Sci Technol 53(1):50–59. https://doi.org/10.1021/acs.est.8b04673
Li X, Chen D, Carrión VJ, Revillini D, Yin S, Dong Y, Zhang T, Wang X, Delgado-Baquerizo M (2023) Acidification suppresses the natural capacity of soil microbiome to fight pathogenic Fusarium infections. Nat Commun 14(1):5090. https://doi.org/10.1038/s41467-023-40810-z
Liu J, Shu A, Song W, Shi W, Li M, Zhang W, Li Z, Liu G, Yuan F, Zhang S, Liu Z, Gao Z (2021) Long-term organic fertilizer substitution increases rice yield by improving soil properties and regulating soil bacteria. Geoderma 404:115287. https://doi.org/10.1016/j.geoderma.2021.115287
Liu X, Liu H, Zhang Y, Liu C, Liu Y, Li Z, Zhang M (2023) Organic amendments alter microbiota assembly to stimulate soil metabolism for improving soil quality in wheat-maize rotation system. J Environ Manage 339:117927. https://doi.org/10.1016/j.jenvman.2023.117927
Lombard V, Bernard T, Rancurel C, Brumer H, Coutinho PM, Henrissat B (2010) A hierarchical classification of polysaccharide lyases for glycogenomics. Biochem J 432(3):437–444. https://doi.org/10.1042/BJ20101185
Louca S, Polz MF, Mazel F, Albright MBN, Huber JA, O'Connor MI, Ackermann M, Hahn AS, Srivastava DS, Crowe SA, Doebeli M, Parfrey LW (2018) Function and functional redundancy in microbial systems. Nat Ecol Evol 2(6):936–943. https://doi.org/10.1038/s41559-018-0519-1
Murphy J, Riley JP (1962) A modified single solution method for the determination of phosphate in natural waters. Anal Chim Acta 27:31–36. https://doi.org/10.1016/S0003-2670(00)88444-5
Nayfach S, Camargo AP, Schulz F, Eloe-Fadrosh E, Roux S, Kyrpides NC (2021) Checkv assesses the quality and completeness of metagenome-assembled viral genomes. Nat Biotechnol 39(5):578–585. https://doi.org/10.1038/s41587-020-00774-7
Neira G, Vergara E, Holmes DS (2022) Genome-guided prediction of acid resistance mechanisms in acidophilic methanotrophs of phylogenetically deep-rooted Verrucomicrobia isolated from geothermal environments. Front Microbiol. https://doi.org/10.3389/fmicb.2022.900531
Nicholson FA, Chambers BJ, Williams JR, Unwin RJ (1999) Heavy metal contents of livestock feeds and animal manures in England and Wales. Bioresource Technol 70(1):23–31. https://doi.org/10.1016/S0960-8524(99)00017-6
Palansooriya KN, Wong JTF, Hashimoto Y, Huang L, Rinklebe J, Chang SX, Bolan N, Wang H, Ok YS (2019) Response of microbial communities to biochar-amended soils: a critical review. Biochar 1(1):3–22. https://doi.org/10.1007/s42773-019-00009-2
Pasternak K, Kocot J, Horecka A (2010) Biochemistry of magnesium. J Elem 15(3):601–616. https://doi.org/10.5601/jelem.2010.15.3.601-616
Ren C, Zhang X, Zhang S, Wang JY, Xu M, Guo Y, Wang J, Han X, Zhao F, Yang G, Doughty R (2021) Altered microbial CAZyme families indicated dead biomass decomposition following afforestation. Soil Biol Biochem 160:108362. https://doi.org/10.1016/j.soilbio.2021.108362
Santos-Medellin C, Zinke LA, ter Horst AM, Gelardi DL, Parikh SJ, Emerson JB (2021) Viromes outperform total metagenomes in revealing the spatiotemporal patterns of agricultural soil viral communities. ISME J 15(7):1956–1970. https://doi.org/10.1038/s41396-021-00897-y
Santos-Medellín C, Estera-Molina K, Yuan M, Pett-Ridge J, Firestone MK, Emerson JB (2022) Spatial turnover of soil viral populations and genotypes overlain by cohesive responses to moisture in grasslands. Proc Natl Acad Sci 119(45):e2209132119. https://doi.org/10.1073/pnas.2209132119
Shang J, Sun Y (2022) CHERRY: a computational method for accurate prediction of virus-prokaryotic interactions using a graph encoder-decoder model. Brief Bioinform 23(5):bbac182. https://doi.org/10.1093/bib/bbac182
Singh H, Northup BK, Rice CW, Prasad PVV (2022) Biochar applications influence soil physical and chemical properties, microbial diversity, and crop productivity: a meta-analysis. Biochar 4(1):8. https://doi.org/10.1007/s42773-022-00138-1
Stegen JC, Lin X, Fredrickson JK, Chen X, Kennedy DW, Murray CJ, Rockhold ML, Konopka A (2013) Quantifying community assembly processes and identifying features that impose them. ISME J 7(11):2069–2079. https://doi.org/10.1038/ismej.2013.93
Steinegger M, Söding J (2018) Clustering huge protein sequence sets in linear time. Nat Commun 9(1):2542. https://doi.org/10.1038/s41467-018-04964-5
Sun Q, Zhang Q, Huang Z, Wei C, Li Y, Xu H (2024) Effect of organic fertilizer application on microbial community regulation and pollutant accumulation in typical red soil in South China. Agronomy 14(9):2150. https://doi.org/10.3390/agronomy14092150
Trivedi P, Leach JE, Tringe SG, Sa T, Singh BK (2020) Plant-microbiome interactions: from community assembly to plant health. Nat Rev Microbiol 18(11):607–621. https://doi.org/10.1038/s41579-020-0412-1
Tyc O, Song C, Dickschat JS, Vos M, Garbeva P (2017) The ecological role of volatile and soluble secondary metabolites produced by soil bacteria. Trends Microbiol 25(4):280–292. https://doi.org/10.1016/j.tim.2016.12.002
Urgessa TG (2021) Effect of different source and rates of biochar application on selected physic-chemical properties of acidic soil in western ethiopia. Modern Chemistry 9(4):77–82. https://doi.org/10.11648/j.mc.20210904.12
Uchimiya M, Chang S, Klasson KT (2011) Screening biochars for heavy metal retention in soil: role of oxygen functional groups. J Hazard Mater 190(1):432–441. https://doi.org/10.1016/j.jhazmat.2011.03.063
Wang J, Wang S (2019) Preparation, modification and environmental application of biochar: a review. J Clean Prod 227:1002–1022. https://doi.org/10.1016/j.jclepro.2019.04.282
Wang J, Appidi MR, Burdick LH, Abraham PE, Hettich RL, Pelletier DA, Doktycz MJ (2024) Formation of a constructed microbial community in a nutrient-rich environment indicates bacterial interspecific competition. mSystems 9:e00006-24
Wei X, Ge T, Wu C, Wang S, Mason-Jones K, Li Y, Zhu Z, Hu Y, Liang C, Shen J, Wu J, Kuzyakov Y (2021) T4–like phages reveal the potential role of viruses in soil organic matter mineralization. Environmental Science & Technology 55(9):6440–6448. https://doi.org/10.1021/acs.est.0c06014
Wen T, Xie P, Yang S, Niu G, Liu X, Ding Z, Xue C, Liu Y-X, Shen Q, Yuan J (2022) ggClusterNet: an R package for microbiome network analysis and modularity-based multiple network layouts. iMeta 1(3):e32. https://doi.org/10.1002/imt2.32

Withers E, Hill PW, Chadwick DR, Jones DL (2020) Use of untargeted metabolomics for assessing soil quality and microbial function. Soil Biol Biochem 143:107758. https://doi.org/10.1016/j.soilbio.2020.107758

Wong JWC, Fang M (2000) Effects of lime addition on sewage sludge composting process. Water Res 34(15):3691–3698. https://doi.org/10.1016/S0043-1354(00)00116-0

Wu H, Wan S, Ruan C, Niu X, Chen G, Liu Y, Zhu K, Schulin R, Wang G (2022) Phage-bacterium interactions and nutrient availability can shape C and N retention in microbial biomass. Eur J Soil Sci 73(4):e13296. https://doi.org/10.1111/ejss.13296

Yao Y, Gao B, Zhang M, Inyang M, Zimmerman AR (2012) Effect of biochar amendment on sorption and leaching of nitrate, ammonium, and phosphate in a sandy soil. Chemosphere 89(11):1467–1471. https://doi.org/10.1016/j.chemosphere.2012.06.002

Yuan J-H, Xu R-K, Zhang H (2011) The forms of alkalis in the biochar produced from crop residues at different temperatures. Bioresour Technol 102(3):3488–3497. https://doi.org/10.1016/j.biortech.2010.11.018

Zhang M, Zhang L, Riaz M, Xia H, Jiang C (2021) Biochar amendment improved fruit quality and soil properties and microbial communities at different depths in citrus production. J Clean Prod 292:126062. https://doi.org/10.1016/j.jclepro.2021.126062

Zhao J, Qiu YB, Yi F, Li J, Wang X, Fu Q, Fu X, Yao Z, Dai Z, Qiu YP, Chen H (2024) Biochar dose-dependent impacts on soil bacterial and fungal diversity across the globe. Sci Total Environ 930:172509. https://doi.org/10.1016/j.scitotenv.2024.172509

Zheng X, Xu W, Dong J, Yang T, Shangguan Z, Qu J, Li X, Tan X (2022) The effects of biochar and its applications in the microbial remediation of contaminated soil: a review. J Hazard Mater 438:129557. https://doi.org/10.1016/j.jhazmat.2022.129557

Zhong Y, Yan W, Wang R, Wang W, Shangguan Z (2018) Decreased occurrence of carbon cycle functions in microbial communities along with long-term secondary succession. Soil Biol Biochem 123:207–217. https://doi.org/10.1016/j.soilbio.2018.05.017

Zhou G, Chen L, Zhang C, Ma D, Zhang J (2023) Bacteria-virus interactions are more crucial in soil organic carbon storage than iron protection in biochar-amended paddy soils. Environ Sci Technol 57(48):19713–19722. https://doi.org/10.1021/acs.est.3c04398

Zhu X, Chen B, Zhu L, Xing B (2017) Effects and mechanisms of biochar-microbe interactions in soil improvement and pollution remediation: a review. Environ Pollut 227:98–115. https://doi.org/10.1016/j.envpol.2017.04.032